Transportation Research Part C 87 (2018) 138–158

Contents lists available at ScienceDirect

Transportation Research Part C

journal homepage: www.elsevier.com/locate/trc

Region-based prescriptive route guidance for travelers of multiple classes

Antonis F. Lentzakis*, Simon I. Ware, Rong Su, Changyun Wen

School of Electrical and Electronic Engineering, Nanyang Technological University, 50 Nanyang Avenue, Singapore

ARTICLE INFO

Keywords:
Urban traffic management
Route guidance
Autonomous vehicles
Dynamic traffic modeling

ABSTRACT

The performance and complicated interactions of different classes of travelers on regional urban networks are presented and analyzed. A new multi-class extension of a regional dynamic traffic model, the Network Transmission Model is proposed. The classes in question correspond to travelers using autonomous vehicles, conventional vehicles, equipped with Route Guidance and Information Systems, and unequipped vehicles. Each class is represented by a different routing method. Incremental Route Planning, an innovative predictive simulation-based routing method, Proxy Regret Matching, a non-predictive strategic learning-based method and Multinomial Logit-based Routing for 1st, 2nd and 3rd class respectively. All routing methods include a Public Transit Diversion mechanism and are assumed to provide prescriptive route guidance, with pre-trip information dissemination for every departing vehicle. We consider the possibility of non-compliance for conventional vehicles equipped with Route Guidance and Information Systems. We also consider 2 possible scenarios for autonomous vehicles that affect their travel time prediction accuracy. We simulate regional traffic dynamics for simultaneous application of all aforementioned routing methods, employing a market penetration scheme for each class of travelers. We analyze results regarding the overall network performance for various combinations of traveler class market penetration rates and non-compliance rates. We come to the conclusion that autonomous vehicles will not only provide benefits for 1st class travelers, but for all traveler classes on the network.

1. Introduction

Quality of life in cities, especially for vehicle passengers, can be directly attributed to the delay they experience daily, as a consequence of congestion. Traffic congestion can be caused by temporary deterioration of network performance, in case of an incident. There can also be recurrent congestion, whereby the travel demand bound for certain regions within the urban traffic network exceeds the capacity of said regions, for specific time periods. Due to limited space availability in modern urban areas, costs associated with infrastructure upgrade and extension are prohibitive. Optimizing the supply of existing infrastructure resources, through use of traffic light control (Papageorgiou et al., 2003; Kuyer et al., 2008; Aboudolas et al., 2009; Haddad et al., 2013), route guidance (Garcia et al., 2000; Knoop et al., 2012; Hajiahmadi et al., 2013; Yildirimoglu et al., 2015), as well as restricting network travel demand through toll pricing (Geroliminis and Levinson, 2009; Zheng et al., 2012, 2016; Simoni et al., 2015), at different degrees of granularity (individual network links, subnetworks), can help alleviate congestion phenomena. Integration of intelligent sensor technologies, such as RSU (Road Side Unites) with DSRC (Dedicated Short Range Communications) capability, to the network infrastructure can help increase the performance of the methods used to increase network capacity or restrict network travel demand,

* Corresponding author.
E-mail address: antonios001@e.ntu.edu.sg (A.F. Lentzakis).

https://doi.org/10.1016/j.trc.2018.01.006
Received 21 November 2016; Received in revised form 4 January 2018; Accepted 4 January 2018

especially during peak hour.

In the not-so-distant future, self-driving cars are expected to comprise a significant portion of the vehicle population in metropolitan areas, more concretely, experts are forecasting a 70% market penetration rate for autonomous vehicles by 2040 (IEEE, 2012). One of the main driving forces behind autonomous vehicle technology adoption is the improvement of passenger safety through elimination of human error. Human error accounts for 94% of road accidents (Dingus et al., 2016), which in turn account for 10–30% of delays due to congestion (Skabardonis et al., 2003). One of the main obstacles facing the adoption of autonomous vehicles is the uncertainty regarding their successful integration in human driver-populated traffic networks. Conventional vehicles equipped with navigation devices are able to receive several types of guidance. Descriptive guidance involves prevailing traffic conditions, predicted travel times and incident information. Prescriptive guidance involves specific shortest route information provision. Route guidance can provide user-oriented benefits. Given that vehicles remain compliant to their prescribed routes (Hoogendoorn and Bovy, 1998), route guidance can also lead to system-wide near-optimal network performance. Autonomous vehicles are expected to always maintain compliance, and through coordination with traffic control centers, can lead to system-wide benefits. Past research into the adoption and potential impact of autonomous vehicles has prioritized highly detailed dynamic modeling and simulation (Fagnant and Kockelman (2014), Katrakazas et al. (2015), Talebpour and Mahmassani (2016), Wang et al. (2017)). Region-based routing can be considered as routing at an aggregated level. Any large urban traffic network can be appropriately partitioned into regions (Ji and Geroliminis, 2012; Lentzakis et al., 2014; Etemadnia et al., 2014; Saeedmanesh and Geroliminis, 2016, 2017). Region-based routing then presents a set of region sequences that drivers can follow from their origin region to their desired destination region. This has been shown to lead to significant decrease of total vehicle travel time and better utilization of available resources, i.e. the regions of the urban traffic network, in our previous work (Lentzakis et al., 2016). In transportation economics literature, travelers are classified into certain broad categories, according to their value of time, type of activity (commuting to work, leisure) or other criteria and are given the option of changing their desired departure times, which becomes an additional control parameter (Small and Verhoef, 2007). However, this classification introduces additional complexity and stochasticity to the route selection process. In addition, many studies fail to consider the bounded rationality of travelers as decision makers (van Essen et al., 2016). A public transit diversion mechanism, as integrated to each routing method presented in this paper, can be considered as an alternative route choice which does not compromise travelers' departure time preferences. This feature would not be as readily justifiable in a link-by-link routing approach, where the destination location might be a considerable distance away from a public transit station.

1.1. Background on macroscopic fundamental diagram

Godfrey (1969) first proposed the existence of a Macroscopic Fundamental Diagram representing the relationship between vehicle density (veh/km) and space-mean flow (veh/h) for urban regions. Herman and Prigogine (1979) defined a Two Fluid Kinetic model later improved upon by Herman and Ardekani (1984) that stated that the average speed in urban network traffic is a function of the ratio of stopped vehicles, which can be represented as a power function of network link density. Daganzo (2007) defined a relationship between urban network output, representing the number of trips ending inside or outside of the network, and number of vehicles present at the network, or accumulation. This relationship should be valid under the condition that congestion is distributed in a homogeneous fashion throughout the network and as long as external conditions are varying at a slow rate. Geroliminis and Daganzo (2007) posited that the Macroscopic Fundamental Diagram can also exist for urban areas. The Macroscopic Fundamental Diagram, MFD for brevity, has been a staple of freeway traffic modeling and applications, but it's accuracy, as regards freeway networks, has recently been called into question (Mahmassani and Saberi, 2013; Geroliminis and Sun, 2011a; Knoop and Hoogendoorn, 2013). The MFD has been shown to be a suitable modeling tool for urban network regions, characterized by low intra-regional link density variability. The Urban-scale MFD can relate the number of vehicles within a certain region, called accumulation, to the product of average network flow and length, called production. The Urban-scale MFD presents in the shape of a asymmetric unimodal concave function, where for a critical accumulation value, network production is at capacity. For accumulation values below the critical value, network is considered to be under free flow conditions, while for accumulation values above the critical value, network is considered to be congested, ranging from lightly congested, all the way to gridlock. A well-defined Urban-scale MFD can only exist under homogeneous distribution of congestion. The traffic modeling of a network partitioned to several regions each represented with a MFD is first developed in Geroliminis et al. (2013). Geroliminis and Sun (2011b), Mazloumian et al. (2010) and Daganzo et al. (2011) have demonstrated the importance of network link density variability in acquiring a well-defined Urban-scale MFD. Additionally, work from de Jong et al. (2013), Leclercq and Geroliminis (2013), Knoop et al. (2014), Gayah et al. (2014) indicates that network topology, traffic signal settings, route distribution and demand can actually affect the total output of a region. Leclercq et al. (2015) posited that MFD shape will change when for the same network, different route distribution is applied and proposed a framework whereby all routes within a region would be grouped into macroscopic route clusters. Keyvan-Ekbatani et al. (2016) found that the integration of adaptive traffic control and network gating leads to higher network throughput as well as shorter queues on the boundary expanding work by Gayah et al. (2014). There are two approaches in mitigating these effects. One approach is to incorporate link density variability, a measure of congestion heterogeneity, in the relationship defined by the Urban-scale MFD, deriving an MFD dependent not only on the accumulation, but also link density variability, as in Simoni et al. (2015), Ramezani et al. (2015), Yildirimoglu et al. (2015). Another approach is to partition the urban traffic network into homogeneously congested regions with well-defined Urban-scale MFDs. Examples of different partitioning schemes resulting in homogeneously congested regions can be found in Ji and Geroliminis (2012), Lentzakis et al. (2014), Ji et al. (2014), Saeedmanesh and Geroliminis (2016). One of several regional dynamic traffic models used to describe region-based traffic dynamics, the Network Transmission Model, NTM for short, was originally developed by Knoop and Hoogendoorn (2014, 2015) and later implemented in a real-world application by Knoop et al.

(2016). The NTM describes a multi-layer network that comprises of a regional and an urban traffic layer and takes into account the dynamics of a network as expressed through the Urban-scale MFD, to implement a demand and supply scheme between regions with capacitated boundaries, similar to the Cell Transmission Model by Daganzo (1994). The concept of Urban-scale MFD has been used extensively in research into perimeter control schemes (Aboudolas and Geroliminis, 2013; Haddad et al., 2012; Keyvan-Ekbatani et al., 2012, 2013, 2015; Haddad and Mirkin, 2017; Kouvelas et al., 2017), pricing (Geroliminis and Levinson, 2009; Zheng et al., 2012; Simoni et al., 2015; Zheng et al., 2016), but to a lesser extent in routing applications (Knoop et al., 2012; Hajiahmadi et al., 2013; Yildirimoglu et al., 2015; Lentzakis et al., 2016; Xiong et al., 2016). Recently, efforts have been made to combine link-based and aggregate traffic modeling for MFD-based control approaches (Zheng et al., 2012; Keyvan-Ekbatani et al., 2016). Investigations into combined types of traffic management have also gained traction in the researcher community (Papageorgiou and Messmer, 1991; Chen and Ben-Akiva, 1998; Yang, 1999; Adler et al., 2005; de Cea Ch and Valverde, 2009). Sirmatel and Geroliminis (2016) are the first to combine route guidance and perimeter control as part of an MFD-based traffic management scheme. A significant part of transportation is classification of the travel demand into multiple modes, however most of the MFD-based traffic literature have been focusing on the public transport aspect of multi-modal travel demand modeling and management (buses, trams) (Ampountolas et al., 2014; Zheng et al., 2013; Geroliminis et al., 2014; Chiabaut, 2015; Ortigosa et al., 2015, 2017; Yildirimoglu et al., 2016), however, there has been, to the authors' knowledge, no research into a framework that integrates autonomous vehicles into a private ownership or ridesharing scheme.

1.2. Objectives and contributions

In this work, we introduce and implement a multi-class extension of a region-based dynamic traffic model called Network Transmission Model, which marks the first contribution of this paper. Subsequently, we apply individually, as well as in various combinations, different types of routing approaches. We introduce a predictive simulation-based routing approach called Incremental Route Planning, as an additional contribution of this paper. The purpose of this mixed application of different types of route guidance, which marks the main contribution of this paper, is to showcase the interaction of different traveler classes, on a regional traffic network. Each class features distinct characteristics and is being represented by different types of route guidance. We first define 3 distinct traveler classes, a class of travelers equipped with autonomous vehicles, a traveler class comprising of human-driven vehicles equipped with a route guidance and information system and a traveler class comprising of human-driven vehicles without any sort of navigation equipment. The 1st traveler class is assumed to be fully compliant, while the 2nd traveler class may include non-compliant human drivers, which would be subsumed in the 3rd class of travelers. We will compare prescriptive pre-trip guidance approaches, including a predictive simulation-based approach, Incremental Route Planning (IRP), which comprises 2 steps, forecasting and path set computation/assignment, for the 1st traveler class, and Proxy Regret Matching (PRM), a non-predictive strategic learning-based approach, which provides a distribution of regional paths to be assigned based on their estimated average regret, for the compliant segment of the 2nd traveler class. Finally, we implement an extended version of Multinomial Logit-based Routing (MLR), which gives the multinomial logit-based Dynamic Stochastic User Equilibrium, DSUE for brevity, representing a more realistic route choice behavior for the non-compliant segment of the 2nd traveler class and the 3rd traveler class of unequipped human-driven vehicles, both characterized by imperfect travel time perception, which informs travelers' decision at the time of departure in such a way, that no unilateral deviation will lead to a decrease in their imperfectly perceived travel time. Yildirimoglu and Geroliminis (2014) introduced a region-based Dynamic Traffic Assignment model for a regional network and achieved DSUE conditions through implementation of the Method of Successive Averages, MSA, for brevity. They were able to demonstrate that congestion was accurately described by developed regional dynamics with results similar to link-based dynamics, which otherwise might be unavailable. Yildirimoglu et al. (2015), inspired by Ramezani et al. (2015), extended their work by introducing heterogeneity in the MFD-based traffic model, as well as the option to have paths containing the same region more than once and most importantly route guidance based on Dynamic System Optimum regional flow distribution. However, their method was not intended as a traffic management strategy for too many regions. Our framework focuses on computational efficiency. While MSA takes overlapping paths into consideration, a noted weakness of the Multinomial Logit-based Routing model, at a regional setting, path overlap is not a deciding factor. We consider 2 distinct market penetration rates, one for the adoption of private autonomous vehicles as the primary mode of transport, assigned to the 1st traveler class (MPR1), and one for the equipment of route guidance information systems utilizing strategic learning-based routing assigned to the 2nd traveler class (MPR2). Subsequently, after the respective market penetration rates for the different traveler classes have been set, we define a rate of non-compliance (NC) for the 2nd class of human-driven vehicles and group the non-compliant segment together with the remainder of the vehicle population, classified as the 3rd traveler class, resulting in rate (MPR3). The diagram shown in Fig. 1 depicts the aforementioned classification process.

The rest of this paper is organized in the following manner. In Section 2, we present a multi-class extension of the Network Transmission Model, a region-based dynamic traffic model that employs the Urban-scale MFD to accurately describe the traffic dynamics for homogeneously congested regions. In Section 3, we present an extension of a multinomial logit-based routing approach, a non-predictive routing approach which employs proxy regret matching, and introduce a predictive routing approach which employs simulation-based forecasting. We also introduce a market penetration scheme for all aforementioned routing approaches. In Section 4 we present our network setup. We then use our simulation results to compare the performance of each approach applied separately to our network setup. We subsequently test for a wide range of market penetration rate combinations, whereupon we apply the respective routing approaches to the network simultaneously and comment on the performance results. In Section 5 we present our conclusions and possible future work.

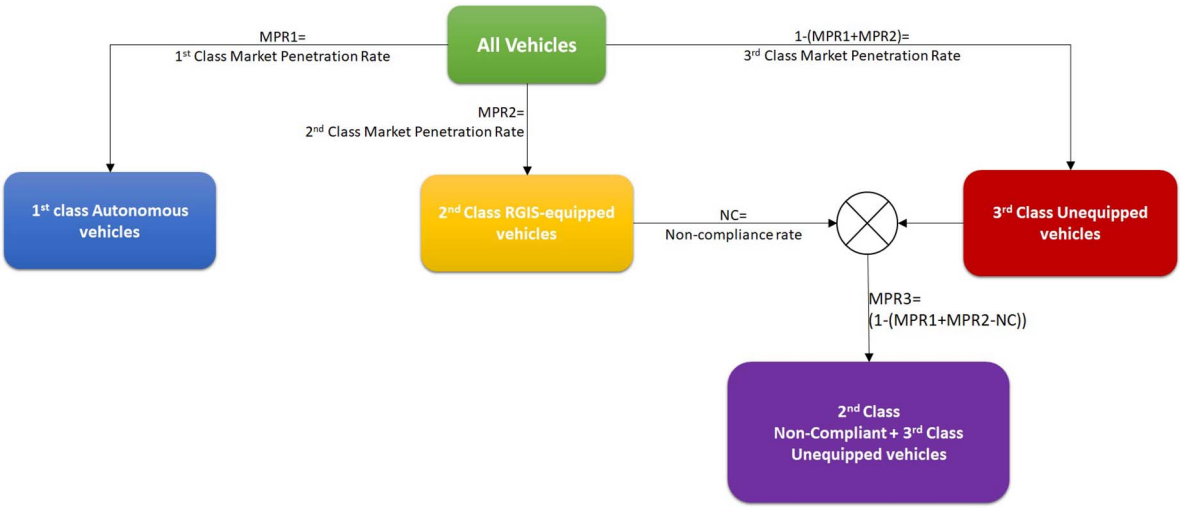

Fig. 1. Process of assigning vehicle population to multiple traveler classes.

2. Multi-class network transmission model

In this section, we introduce our multi-class extension of the Network Transmission Model, originally developed by Knoop and Hoogendoorn (2014) and most recently implemented and validated by Knoop et al. (2016) in the real world city of the Hague. In Section 2.1, we provide the notation and terminologies used in our model. In Section 2.2, we provide a description of the multi-class regional traffic model.

2.1. Notations and terminologies

Let a directed graph $G = (K,A)$ denote the regional traffic network, which comprises a set of regions $\mathscr{K}$ and a set of interregional boundaries $\mathscr{A}$. The following notations will be used to describe our multi-class extension of the NTM:

Sets:
- $\mathscr{K}$: set of nodes, $|\mathscr{K}| = m$, representing homogeneous regions;
- $\mathscr{A} \subseteq \mathscr{K} \times \mathscr{K}$: set of arcs, $|\mathscr{A}| = l$, representing interregional boundaries;
- $\mathscr{K}_o \subset \mathscr{K}$: set of origins, $|\mathscr{K}_o| = o$;
- $\mathscr{K}_d \subset \mathscr{K}$: set of destinations, $|\mathscr{K}_d| = d$;
- $C = [c_{i,j}]^{m\times m} \geqslant 0, c_{i,j} > 0 \Leftrightarrow (i,j) \in \mathscr{A}$, the boundary capacity matrix;
- $\mathscr{P}_{b,e}$: set of all paths from origin b to destination e ,$\forall\ b \in \mathscr{K}_o$,$\forall\ e \in \mathscr{K}_d$;
- $\mathscr{P}_e := \bigcup_{b\in\mathscr{K}_o} \mathscr{P}_{b,e}$, set of all paths with destination e ,$\forall\ b \in \mathscr{K}_o$;
- $\mathscr{P}_b := \bigcup_{e\in\mathscr{K}_d} \mathscr{P}_{b,e}$, set of all paths with origin b ,$\forall\ e \in \mathscr{K}_d$;
- $\mathscr{P} := \mathscr{P}_b \bigcup \mathscr{P}_e$, set of all possible paths;
- Ω: set of classes, representing different types of travelers;
- $\mathscr{Z}_i$: the set of links in region $i \in \mathscr{K}$;
- $\mathscr{H}$: set of discrete time steps.

Index variables:
- $i,j \in \mathscr{K}$: region indices, where $(i,j) \in \mathscr{A}$, i.e., region i is adjacent to j;
- $b \in \mathscr{K}_o$: origin region index;
- $e \in \mathscr{K}_d$: destination region index;
- $p \in \mathscr{P}_{b,e}$: path from origin b to destination e;
- $\omega \in \Omega$: traveler class index;
- $z \in \mathscr{Z}_i$: link that belongs to region i;
- $h \in \mathscr{H}$: discrete time index.

Traffic network parameters:
- $v_{i,f} \in \mathbb{R}^+$: average speed (km/h) for region i under free-flow conditions;
- $n_{i,crit} \in \mathbb{R}^+$: critical accumulation (veh) for region i;
- $Q_{i,crit} \in \mathbb{R}^+$: average network flow (veh·m/h) for region i at capacity flow;
- λ_z: number of lanes on link $z \in \mathscr{Z}_i$;
- Λ_z: length of link $z \in \mathscr{Z}_i$;
- T_H: simulation time (s);

T_s: sample time (s);
$H = \lfloor T_H/T_s \rfloor$: simulation horizon.
Traffic state variables:
$n_z(h)$: number of vehicles on link $z \in \mathscr{Z}_i$ at step h;
$n_i(h) = \sum_{z\in\mathscr{Z}_i} n_z(h)$, accumulation in region i i at step h;
$n^{\omega}_{i,b,e}(h)$: ω-class, b-origin, e-destination specific accumulation in region i at step h;
$\zeta^{\omega}_{b,e}(h)$: ω-class, b-origin, e-destination specific travel demand at departure time step h;
$\zeta_{b,e}(h) = \sum_{\omega\in\Omega} \zeta^{\omega}_{b,e}(h)$: b-origin, e-destination specific travel demand at departure time step h;
$Q_i(n_i(h))$: approximation function to the Urban-scale MFD, according to Drake et al. (1967);
$v_i(n_i(h))$: average network speed approximation function, according to Drake et al. (1967);
$P_j(h)$: representing the supply, similar to Knoop and Hoogendoorn (2015);
$\beta^{p,\omega}_{i,j,b,e}(h)$: p-path, ω-class, b-origin, e-destination specific branching rates from region i to j, at step h, where $p \in \mathscr{P}_{b,e}$
$Z_{i,j}(h)$: unrestricted demand from region i to j at step h;
$\widetilde{Z}_{i,j}(h)$: effective demand from region i to j at step h;
$\widetilde{Z}^{\omega}_{i,j,b,e}(h)$: ω-class, b-origin, e-destination specific demand from region i to j at step h;
$Z_j(h)$: total demand to region j at step h;
$\epsilon_j(h)$: the flow proportion that can travel into region j;
$\chi_i(h)$: the minimum of the exit flow proportions;
$q_{i,j}(h)$: outgoing flow from region i to j at step h;
$q^{\omega}_{i,j,b,e}(h) = \chi_i(h)\widetilde{Z}^{\omega}_{i,j,b,e}(h)$: ω-class,b-origin, e-destination specific outgoing flow from region i to j at step h.

2.2. Model description

In order to describe region-based traffic dynamics, we introduce a multi-class extension the NTM (Network Transmission Model). The NTM describes a traffic network at the urban traffic level as well as at the aggregated regional traffic level. NTM takes into account the dynamics of a network as expressed through the Urban-scale MFD, as well as the limited capacity of the boundaries between regions (Knoop and Hoogendoorn, 2015). The NTM combines the concepts of the Cell Transmission Model by Daganzo (1994), CTM for brevity, and a node model by Jin and Zhang (2003) and applies it to a model describing urban traffic network dynamics at a regional level. Unlike the regional dynamic traffic model developed by Geroliminis et al. (2013) that explicitly models internal traffic demand, NTM accounts for internal traffic demand implicitly. Concretely, while, for a supply/demand scheme, regional supply values work similarly to Daganzo's CTM, regional demand values follow the curve of a regional performance function, an abstraction of a link performance function, corresponding to a scaled-down Urban-scale MFD (Gonzales, 2015). It should be noted that, even though this modeling approach omits explicit modeling of uncontrollable internal flows, leading to faster, if less accurate, analysis of the traffic management effects on the network, it also presents with some limitations, which might inhibit adoption in real-life applications with high accuracy requirements. It is worth mentioning that, when it comes to model accuracy, explicit modeling of internal flows, as is the case in the framework of Geroliminis et al. (2013), as well as works extending said framework, see Haddad and Shraiber (2014), Ramezani et al. (2015), Yildirimoglu et al. (2015), is the superior modeling methodology. Our multi-class extension introduces class/origin/destination specific accumulations, as well as pre-trip information in the form of regional path/class branching rates for each respective origin/destination pair, adjusting the traffic dynamics accordingly. As mentioned in the previous section, in our case, classes refer to travelers represented by different types of routing approaches. In short, the dynamics of each region $i \in \mathscr{K}$ are described as follows:

$$n_i(h+1) = \sum_{e\in\mathscr{K}_d} \sum_{b\in\mathscr{K}_o} \sum_{\omega\in\Omega} n^{\omega}_{i,b,e}(h+1), \tag{1}$$

where total accumulation $n_i(h+1)$ for region i at step $h+1$ comprises all ω-class, b-origin, e-destination specific accumulations $n^{\omega}_{i,b,e}(h+1)$, which in turn can be derived from the following dynamic equation:

$$n^{\omega}_{i,b,e}(h+1) = n^{\omega}_{i,b,e}(h) + \frac{T_s}{\sum_{z\in\mathscr{Z}_i} \lambda_z \Lambda_z} \left(\sum_{j\in\mathscr{K},(i,j)\in\mathscr{A}} q^{\omega}_{j,i,b,e}(h) - \sum_{j\in\mathscr{K},(i,j)\in\mathscr{A}} q^{\omega}_{i,j,b,e}(h) \right) \tag{2}$$

where $q^{\omega}_{j,i,b,e}(h)$ and $q^{\omega}_{i,j,b,e}(h)$ are the incoming and outgoing flow rates, respectively, for class ω, with origin b and destination e, at step h. More concretely, the urban traffic network is first partitioned into homogeneously congested regions and we derive the Urban-scale MFD for each region. Partitioning into homogeneously congested regions has been investigated extensively in the last 5 years, starting with the seminal paper by Ji and Geroliminis (2012) and followed by several others (Ji et al., 2014; Lentzakis et al., 2014; Saeedmanesh and Geroliminis, 2016, 2017). Both simulation-based and real-life datasets have been used to derive homogeneously congested regions, either statically or dynamically. As mentioned previously, Geroliminis et al. (2013) developed a regional dynamic traffic model, which was extended in Yildirimoglu and Geroliminis (2014), Ramezani et al. (2015), Yildirimoglu et al. (2015) to model and control for heterogeneity in MFD at the regional level. However, Ramezani et al. (2015) and Yildirimoglu et al. (2015) perform a secondary partition of each heterogeneous region into homogeneous subregions, where MFD functions are assumed to be dependent only on the subregional accumulation. In our case, we would select an appropriate partitioning implementation,

dependent on the type of data available, as well as other parameters of our given network, so as to achieve the best possible results for two features, intraregional link density variability and regional compactness and cohesion. In our multi-class extension of the NTM, we have selected to represent the Urban-scale MFDs with an approximation function according to Drake et al. (1967). Specifically, the Urban-scale MFD of region i with accumulation n_i, free speed $v_{i,f}$ and critical accumulation value $n_{i,crit}$, is

$$Q_i(n_i(h)) = n_i(h)v_{i,f}\exp\left(-\xi\left(\frac{n_i(h)}{n_{i,crit}}\right)^{\alpha}\right) \tag{3}$$

Drake et al. (1967) also provide an average network speed approximation function,

$$v_i(n_i(h)) = v_{i,f}\exp\left(-\xi\left(\frac{n_i(h)}{n_{i,crit}}\right)^{\alpha}\right), \tag{4}$$

which is used to derive regional travel times. In literature, several simplistic approximations of MFDs in the form of triangular or trapezoid functions appear for theoretical examples (Daganzo et al., 2011; Gayah et al., 2014) and even some real-life applications Knoop et al. (2016). In recent literature (Geroliminis et al., 2013; Knoop and Hoogendoorn, 2013; Ramezani et al., 2015), 3rd order polynomial functions whose coefficients are tuned based on real-life data have been shown to be more accurate approximations for MFDs of specific regions. The approximation function by Drake et al. (1967) provides a good compromise between accuracy and computational effort. These approximation functions have been shown to be suitable for describing the dynamics of regional traffic networks (Dixit et al., 2007; Knoop et al., 2012; Hajiahmadi et al., 2013). Following (Knoop et al., 2012; Hajiahmadi et al., 2013), we set $\xi = 0.5$ and $\alpha = 2$, however ξ,α can be amenable to tuning, to better fit the Urban-scale MFD derived from real-life data. The interregional flow at each stage is determined by the Urban-scale MFD, separated in demand (unrestricted)

$$Z_{i,j}(h) = \frac{1}{n_i(h)}\sum_{e\in\mathscr{K}_d}\left(\sum_{b\in\mathscr{K}_o}\left(\sum_{\omega\in\Omega}\left(n^{\omega}_{i,b,e}(h)\sum_{p\in\mathscr{P}_{b,e}}\beta^{p,\omega}_{i,j,b,e}(h)Q_i(n_i(h))\right)\right)\right) \tag{5}$$

and supply

$$P_j(h) = \begin{cases} Q_{j,crit} & \text{if } n_j(h) \leqslant n_{j,crit} \\ Q_j(n_j(h)) & \text{if } n_j(h) > n_{j,crit} \end{cases} \tag{6}$$

where regions $i,j \in \mathscr{K}$,$(i,j) \in \mathscr{A}$, at step h. In this supply/demand formulation, supply $P_j(h)$ and total demand $Z_j(h)$ for region j at step h, can be described through $Q_j(n_j(h))$ corresponding to the Urban-scale MFD approximation function described above. Then, similarly to CTM, we can consider the supply $P_j(h)$ equal to regional capacity flow $Q_{j,crit}$, when vehicle accumulation $n_i(h)$ is below the critical value $n_{i,crit}$ and equal to the scaled-down Urban-scale MFD otherwise. Unlike the CTM, where demand increases in tandem with the beyond-critical-value increase to cell density, regional demand $Z_{i,j}(h)$ is *reduced* when vehicle accumulation $n_i(h)$ increases beyond $n_{i,crit}$. In this manner, internal traffic demand for each region and the resulting restriction on the regional outgoing flow are taken into consideration indirectly. For the unrestricted demand $Z_{i,j}(h)$, the boundary capacity between two regions also comes into play, resulting in effective demand

$$\widetilde{Z}_{i,j}(h) = \min\{Z_{i,j}(h),c_{i,j}\}, \tag{7}$$

from region i to j at step h. Effective demand can be further decomposed into ω-class, b-origin, e-destination specific demands from region i to j at step h in the following manner:

$$\widetilde{Z}^{\omega}_{i,j,b,e}(h) = \frac{1}{n_i(h)}\left(n^{\omega}_{i,b,e}(h)\sum_{p\in\mathscr{P}_{b,e}}\beta^{p,\omega}_{i,j,b,e}(h)\right)Q_i(n_i(h))\left(\frac{\widetilde{Z}_{i,j}(h)}{Z_{i,j}(h)}\right) \tag{8}$$

After consolidating all incoming demands to region j into total demand

$$Z_j(h) = \sum_{i\in\mathscr{K},(i,j)\in\mathscr{A}}\widetilde{Z}_{i,j}(h), \tag{9}$$

we determine the flow proportion that can travel into region j as

$$\epsilon_j(h) = \min_{j\in\mathscr{K},(i,j)\in\mathscr{A}}\left\{\frac{P_j(h)}{Z_j(h)},1\right\} \tag{10}$$

Subsequently, flow proportion

$$\chi_i(k) = \min_{j\in\mathscr{K},(i,j)\in\mathscr{A}}\{\epsilon_j(h)\} \tag{11}$$

will be the same for all demands $Z_{i,j}(h)$, under the assumption that traffic cannot freely transition from region to region, due to spillback events on the boundaries as well as congestion within region i. If the flow is limited by the supply, region j receives flow proportional to the demands converging to j. Tampere et al. (2011) observed that the approach selected by Jin and Zhang (2003),

distributing flows proportional to the demand does not satisfy the conservation of branching rates requirement, however, in a regional macroscopic flow setting, this is not necessary. Outflow from region i to j

$$q_{i,j}(h) = \chi_i(h)\widetilde{Z}_{i,j}(h), \tag{12}$$

which is assumed constant between time steps, is effectively the minimum of supply $P_j(h)$ and demand $Z_{i,j}(h)$.

As described in the above equations, the main characteristic of our multi-class extension of the NTM is that, unlike the inter-regional splitting rates of the original, our control variables are path-class-origin–destination specific branching rates, which allow for path-based, rather than transition-based, assignment. Our problem's pre-trip information dissemination structure, as presented in the following section, is usually amenable to path-based route assignment (Garcia et al., 2000; Adler et al., 2005; Kaufman et al., 1998). Concretely, in our multi-class dynamic traffic model, route guidance is implemented through control input variables $\beta_{i,j,b,e}^{p,\omega}(h) \in [0,1]$, which represent p-path, ω-class, b-origin, e-destination specific branching rates from region i to j at step h, where $p \in \mathscr{P}_{b,e}, \omega \in \Omega$. Let $\mathscr{B}_{i,b,e}^{p,\omega}$ be the collection of all feasible p-path, b-origin, e-destination specific branching rates in region i, associated with traveler class ω. If a particular traveler class is characterized by non-compliance, as is the case for the 2nd class in our framework, with non-compliance rates $NC \in \mathscr{C}_{NC} = [0,1]$, the effect of the route guidance provided on the resulting traffic patterns cannot be determined analytically. Rather, we can describe the traffic patterns as a stochastic process over a probability space, whose sample space is $\mathscr{B}_{i,b,e}^{p,\omega} \times \mathscr{C}_{NC}$, with an induced event set $\mathscr{F} := 2^{\mathscr{B}_{i,b,e}^{p,\omega}}$, which is a σ-algebra, and a probability map $\mathscr{S}_{i,b,e}^{p,\omega}$. Owing to this stochastic nature of the branching rates for each region, it is extremely difficult, if still possible, to analyze the traffic conditions under different route guidance approaches. For this reason, in this paper we will adopt a simulation-based approach to analyze the impact of three different route guidance approaches on the traffic patterns and overall network performance, i.e., Multinomial Logit Routing, strategic, learning-based routing method utilizing Proxy Regret Matching, and Incremental Route Planning, with different non-compliance rates. It should also be mentioned, that some shortcomings, associated with the NTM, have also become part of our multi-class extension of the NTM. Regarding possible turning restrictions occurring in a NTM implementation (Knoop et al., 2016), our multi-class extension has already addressed the issue, as mentioned earlier, by virtue of replacing interregional splitting rates with path-class-origin-destination specific branching rates, thus preventing the selection of infeasible routes by design. However, while real-life traffic does not immediately disappear from the network once the assigned traveler demand reaches its destination, that does not seem to be the case for NTM and by extension, for our modeling approach. Regarding this issue, for future implementations where added realism is a prerequisite, parking spaces of predetermined capacity can be introduced for each regional destination, to address the unrealistic, instant unloading of traveler demand from the network. This will require explicit modeling of intraregional flows, in a similar manner to Geroliminis et al. (2013), Haddad and Shraiber (2014), Ramezani et al. (2015), Yildirimoglu et al. (2015), to account for the fact that the assigned traveler demand for each destination region exceeds the corresponding parking space capacity. A limitation appears in the regional supply Eq. (6), whose values can be considered conservative, when respective regional accumulation is below the critical value, leading to underutilization of the corresponding region. This limitation could be addressed in future implementations where increased accuracy is expected, by replacing the constant part of the piecewise supply Eq. (6) with a linear or higher-order function and subsequently tuning the coefficients so as to maximize utilization of the corresponding region.

3. Methodological framework for region-based route guidance

Route Guidance and Information Systems' primary objective is to improve drivers' route choice by providing information about prevailing traffic conditions (descriptive guidance), or directly prescribing routes which are guaranteed to have reduced travel times (prescriptive guidance). Information about traffic conditions or prescribed routes can be passed along at the beginning of the trip (pre-trip). Drivers can also receive updated information in discrete time intervals en-route to their destination, however, the focus of this work will be on pre-trip information dissemination. For each origin-destination pair, a set of shortest paths is calculated and route choice probabilities are assigned for the routes corresponding to the set of shortest paths. Based on this set of probabilities, a route is appropriately prescribed to each departing traveler, representing the control input of a Route Guidance and Information System. The accuracy of route travel time estimation plays an important role in the drivers' compliance rate with the route guidance system. If the route travel time estimation is based on currently prevailing or past traffic conditions, the guidance provided is considered non-predictive. The majority of RGIS (Route Guidance and Information Systems) in use today employ non-predictive guidance. Predictive route guidance employs travel time prediction, based on simulation-based forecasting of traffic conditions. The expected route travel time predicted by the route guidance system will be closer to the experienced route travel time by the drivers than the instantaneous travel time, which is based on current traffic conditions. In this paper, all routing methods presented, including the one introduced in Lentzakis et al. (2016), have been extended to provide the possibility for vehicle passengers to be diverted to public transit, dependent on prevailing or predicted traffic conditions. Following Liu et al. (2009), we assume that public transit capacity can accommodate enough travelers that all public transit routes travel times are constant. For all origin-destination pairs, travel times on public transit routes are assumed to be twice as long as the travel times for the corresponding regional routes, under free flow conditions. This travel time difference takes into consideration possible traveler delays, when changing modes of transport, from private vehicles to public transit.

3.1. Multinomial logit routing with public transit diversion

We first implement an extension of the multinomial logit choice model with Public Transit Diversion integration. Multinomial

Logit Route choice model is used to represent self-interested driver behavior (Sheffi, 1985). This approach provides a Multinomial Logit-based Dynamic Stochastic User Equilibrium (DSUE) for our regional network at every step, which can be used as a more realistic reference case for traveler assignment with imperfect travel time information, during periods of recurrent congestion. We assign a probability to each alternate path μ with travel time TT_μ from a set of κ shortest paths, as follows:

$$P(\mu|\kappa) = \frac{e^{-\vartheta TT_\mu}}{\sum_{\nu\in\kappa} e^{-\vartheta TT_\nu}} \tag{13}$$

where ϑ is a scale parameter associated with travel time uncertainty. It should be noted that the resulting probabilities are sensitive to the units (h, min, s) selected for the travel times. In our case study, sample time is 10 s, hence, $\vartheta = \frac{1}{6}$. We now extend the multinomial logit route choice model to also account for the probability that vehicle passengers will choose to travel by public transit. While we update the shortest path set for every region from the travel times based on the prevailing average speeds $v_i(h)$, the public transit paths from all origins to all destinations are assumed to have constant speed $v_{i,PT} = 0.5v_{i,f}$ and the public transit travel times are calculated accordingly.

3.2. Strategic learning-based route guidance with public transit diversion

We now describe the use of a strategic learning algorithm called Proxy Regret Matching for non-predictive region-based route guidance. This is an extension of the approach used in Lentzakis et al. (2016), with the additional feature of public transit diversion of travelers at the origin, based on prevailing traffic conditions. We consider a repeated game where players, in this case origin regions, are competing for different endpoints, in this case destination regions. The actions are probability distributions over the route choices available for each origin region. For each destination region, at each stage of the repeated game, each origin region (*player*) selects a set of routes (*actions*) ending at said destination, based on an empirical distribution of the player's average past regrets. In a traffic context, these routes are assigned from a RGIS to travelers within the region, according to their destination preferences. In the first step of this routing method, we make use of an algorithm by Yen (1971) to find the sets of k-shortest paths which correspond to the aforementioned route choices. These routes are updated according to the prevailing traffic conditions for each region in the network. Inspired by Lauther (2004), in the second step of this routing method, we implement aggregated regional data preprocessing, so as to increase shortest path calculation efficiency, but most importantly, integrate Public Transit Diversion to our approach. Concretely, for any region $i \in \mathscr{K}$, true (1) or false (0) values are stored in a bit vector $f_{\mathscr{K}} = [f_i]^{m\times 1} \in \{0,1\}, \forall\, i \in \mathscr{K}$. Each vector element f_i is assigned a true (1) value for any region $i|n_i(h) > r_{PRM}\, n_{i,crit}, i \in \mathscr{K}, h \in \mathscr{H}$, with h representing the current time step and r_{PRM} being a threshold coefficient as a percentage of the critical accumulation, allowing for a more or less conservative Public Transit Diversion mechanism. Subsequently, all regions $i|f_i = 1, i \in \mathscr{K}$ are excluded from all k-shortest path set calculations at time step h. If no such path exists, users are diverted to public transit. In the third and final step, we derive the probability distributions for each set of k-shortest paths following the procedure presented below, called Proxy Regret Matching. First we provide some definitions.

3.2.1. Repeated game

In a repeated game, each player tracks their past payoffs and computes the empirical average payoff for each action. Let the origins be the players competing for each of the destinations. A repeated game in a traffic context can then be defined in the following manner, $\forall\, e \in \mathscr{K}_d$:

A repeated game tuple $\langle \mathscr{K}_o, \mathscr{P}_e, U, h\rangle$ where.

- $\mathscr{K}_o$: is the set of players representing the regions designated as origins
- $\mathscr{P}_e := \bigcup_{b\in\mathscr{K}_o} \mathscr{P}_{b,e}$, representing the set of joint actions, where $P_{b,e}$ represents the set of actions available to player $b \in \mathscr{K}_o$. These can be coded as e destination-specific route choices.
- U_b: $\mathscr{P}_e \to \mathbb{R}$ represents the utility function for player i dependent on the joint action of the players
- h represents the current stage of our repeated game

3.2.2. Regret matching

Regret matching algorithms aim to minimize the players' respective regret for their selected actions (Hart and Mas-Colell, 2000). Regret in this context refers to the difference in utility of playing a particular alternative action instead of their currently selected action, given that other players' selected actions are fixed. Players select their actions by drawing from a probability distribution which is proportional to their positive regrets. Regret matching algorithms provide guarantees for convergence of the empirical probability distribution to the set of correlated equilibria, however, said algorithms can be memory intensive, since, each player must keep track of the strategies of all players at every period of play, as well as being able to compute their own utility for changing their strategies during their past plays (Hart and Mas-Colell, 2000). This motivated us to consider Proxy Regret Matching as a less computationally expensive alternative.

3.2.3. Proxy regret matching

Consider now that each player, after each period of play, knows only their own set of actions and their received utility but do not know what is their utility function. They are not aware of what game is being played, i.e. the number of players, their respective actions and payoffs. These are the assumptions of a modified Regret Matching algorithm, called Proxy Regret Matching. For a specific

destination $e \in \mathscr{K}_d$, the average Proxy Regret of player b for $y \in P_{b,e}$ to $z \in P_{b,e}$ at stage h

$$\widehat{M}_b^h(y,z) = \max\left\{\frac{1}{h}\left[\sum_{\eta \leqslant h: p_b^\eta = z} \frac{\sigma_b^\eta(y)}{\sigma_b^\eta(z)} U_b^\eta(p_b^\eta) - \sum_{\eta \leqslant h: p_b^\eta = y} U_i^\eta(p_b^\eta)\right], 0\right\} \tag{14}$$

with $\sum_{y=1}^{P_b} \sigma_b^\eta(y) = 1$, where $\sigma_b^\eta(y)$ denotes the play probability for player $b \in \mathscr{K}_o$ and η denotes the history of plays up to stage h. After calculating the estimated average Proxy Regret, the player adaptively updates the probability of selecting actions to achieve higher utility. If the player selects action y at stage h, the probability of selecting action z at stage $h+1$ is approximately proportional to the average Proxy Regret from y to z. The play probabilities of player b at stage $h+1$ are assigned as follows

$$\sigma_b^{h+1}(z) = \left(1 - \frac{\delta}{h^\gamma}\right)\min\left\{\frac{\widehat{M}_b^h(y,z)}{\mu}, \frac{1}{|P_{b,e}| - 1}\right\} + \frac{\delta}{h^\gamma p_i}, \quad z \neq y,\ z \in P_{b,e} \tag{15}$$

and

$$\sigma_b^{h+1}(y) = 1 - \sum_{w \in P_{b,e}: w \neq x} \sigma_b^{h+1}(w) \tag{16}$$

where $\delta \in [0,1], \gamma < 0.25$ and inertia parameter μ large enough to guarantee that $\sigma_b^{h+1}(y) > 0$.

In this approach, information provision, in the form of past proxy regret distribution, as well as shortest path set assignment, are done in a decentralized manner, even though route selection is implicitly affected by the repeated game's players, in our case the origin regions. It should also be noted that Proxy Regret Matching converges to a distribution of approximate correlated equilibria, however the computational and memory gains more than compensate for the loss in performance.

3.3. Incremental route planning method with public transit diversion

Finally, we will describe our predictive routing method, which is an extension of the dynamic forecast routing method presented in Lentzakis et al. (2016). We present certain definitions and notations necessary for the detailed description of this method, including the time-expanded network representation, first introduced by Ford and Fulkerson (1962). A particularly appealing property of time-expanded networks is their flexibility, allowing for modeling of dynamic travel times dependent on respective regional time-varying demand and/or supply. The size of regional networks, i.e. the number of regions, can implicitly depend on many factors, as the network partitioning scheme is dependent on the Urban-scale MFDs, which in turn can be affected from network topology, traffic signal settings and origin destination demand patterns (Knoop et al., 2014; Gayah et al., 2014). Compared to conventional urban traffic networks, however, regional networks can be at least an order of magnitude smaller. Therefore, concerns regarding the exponential time-expanded network size growth related to the problem input size do not significantly affect regional networks. For the time-expanded networks, we first define a planning horizon $\overline{\mathscr{K}} = \{h_0, h_0 + g, h_0 + 2g, \ldots, h_0 + \Gamma g\}$, where h_0 is the vehicle departure time, g is a small enough interval such that observed traffic conditions vary slowly and Γ a positive integer large enough such that the entire planning horizon is covered. Subsequently, we propose a simulation-based forecasting approach to predictive region-based routing. This approach consists of 2 steps, forecasting and shortest path set computation and assignment. Unlike our non-predictive routing method, the forecasting step of our predictive routing method aggregates prediction information in a centralized manner, while the subsequent shortest path set computation and assignment step is applied locally, for each respective origin destination region pair.

1. The forecasting step involves:
   - Introduction of new vehicles into the regional network based on time-dependent origin-destination Demand Matrix.
   - Simulation of the forward movement of all currently routing vehicles using an extension of the NTM for the regional traffic dynamics, throughout the planning horizon.
   - Virtual vehicle trip generation, starting at the origin regions and assuming route selection according to multinomial logit routing.

     More concretely, we continue the simulation until all vehicles have finished their trips, as well as generate virtual vehicles on origin regions that are assigned trips based on Multinomial Logit routing. Virtual vehicle trip generation allows for more accurate travel time estimation, requiring, however, the computation and assignment of shortest paths to the demand generated at the origin regions. Virtual vehicle trip generation also discourages the frequent use of origin regions as part of the route assignment process.
2. For the shortest path set computation and assignment step:
   - We first expand our original regional network graph $G = (\mathscr{K}, \mathscr{A})$ to a time-expanded network representation $\overline{G} = (\overline{\mathscr{K}}, \overline{\mathscr{A}})$, where $\overline{\mathscr{K}} = \{i^h | i \in \mathscr{K}, h \in \overline{\mathscr{K}}\}$ a set of time-expanded regions and $\overline{\mathscr{A}} = \{(i^h, j^{h'}) | (i,j) \in \mathscr{A}, h + x_{i,j}^h = h', h_0 \leqslant h \leqslant h' \leqslant h_0 + \Gamma g\}$ a set of interregional time-dependent transitions along the set of boundaries $\mathscr{A}$. Weight $x_{i,j}^h \in \mathscr{K}$ is assigned, at time h, for time-expanded regions $i^h, j^{h'} \in \overline{\mathscr{K}}, (i^h, j^{h'}) \in \overline{\mathscr{A}}$, as the number of time steps required for the departing vehicle to transition from region i to j based on the travel times derived during the forecasting step, since the number of steps required for interregional transition are time-varying.

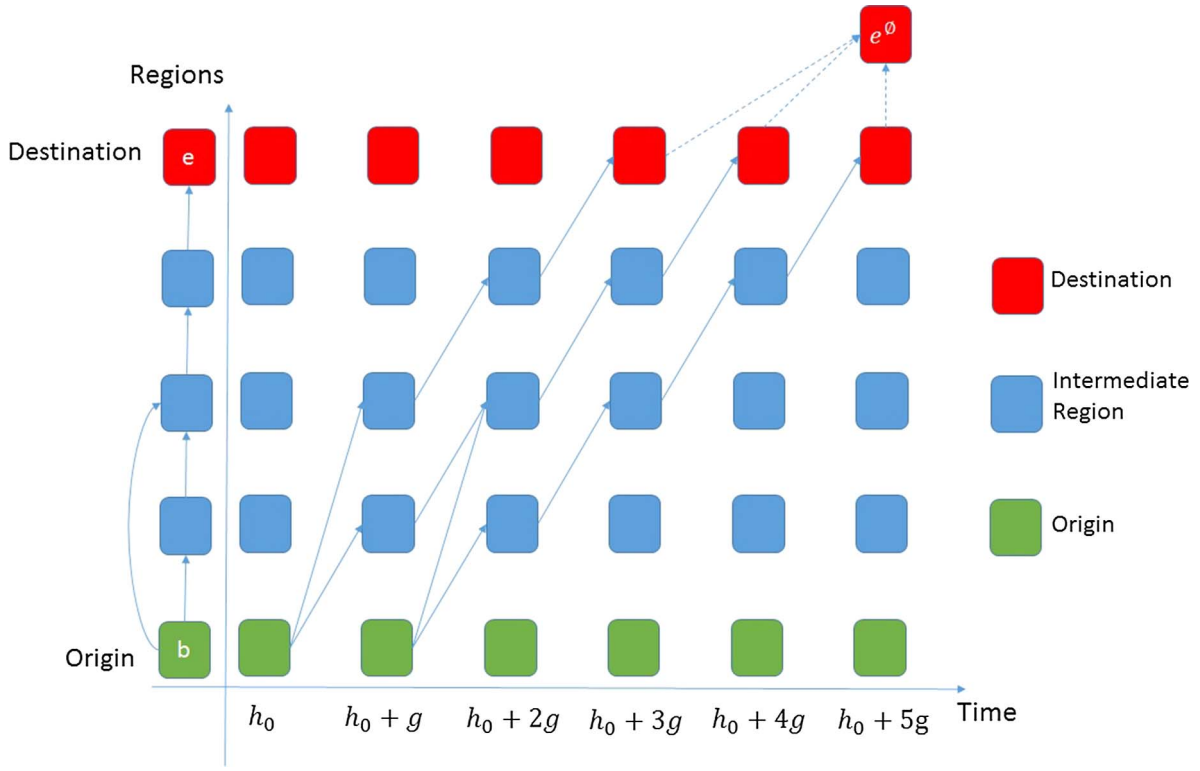

Fig. 2. Time-expanded network representation.

- For each origin region $b \in \mathcal{K}_o$, the discrete time step $h = h_0 + \nu g, \nu \in \mathbb{N}^+$ represents vehicle departure time at origin time-expanded region b^h.For each destination region $e \in \mathcal{K}_d$, the arrival time cannot be predetermined because it is dependent on traffic conditions and the route selected from the κ-shortest paths.So we introduce a dummy destination time-expanded region $e^{\emptyset}$, to represent trip completion with undetermined arrival time $\emptyset$. See Fig.2 for an example.
- The resulting graph $\overline{G}$ contains the set of all eligible paths $\overline{\mathscr{P}}_{b^h,e^{\emptyset}}$ from b^h to $e^{\emptyset}$,$\forall\ b \in \mathcal{K}_o, e \in \mathcal{K}_d$. Similarly to the non-predictive routing approach utilizing Proxy Regret Matching, we implement aggregated regional data preprocessing, utilizing a bit vector $\overline{f}_{\mathcal{K}} = [\overline{f}_i]^{m\times 1} \in \{0,1\}$,$\forall\ i \in \mathcal{K}$ to store true (1) or false (0) values.These vector values represent each region's state of congestion and are similarly used to increase shortest path calculation efficiency, but with one specific difference. If we define $\widetilde{H} = H - h, \Theta = h,\ldots,h + \widetilde{H}$, where h is the current time step, a true (1) value is assigned for any region $i \in \mathcal{K}$, if time-expanded region $i^{\theta} | n_i(\theta) > r_{IRP} n_{i,crit}$,$\forall\ i^{\theta} \in p^{\theta} \in \overline{\mathscr{P}}_{b^{\theta},e^{\emptyset}}, \theta \in \Theta$, where r_{IRP} represents a threshold coefficient as a percentage of the critical accumulation. Subsequently, the set of eligible paths $\overline{\mathscr{P}}_{b^h,e^{\emptyset}}$ contains only regions $i | \overline{f}_i = 0, i \in \mathcal{K}$. If no such path exists, users are diverted to public transit.
- Finally, κ-shortest paths are found by applying an algorithm by Yen (1971) on the modified time-expanded network graph $\overline{G} = (\overline{\mathcal{K}}, \overline{\mathcal{A}})$, which contains only eligible paths. The κ-shortest paths are used to distribute the demand $\zeta_{b,e}(h)$ departing origin b with destination e at time step h.

3.4. Market penetration scheme

In this section, we will focus on mixed application of predictive and non-predictive types of prescriptive route guidance methods with pre-trip information dissemination with the following assumptions:

- In each vehicle, vehicle-integrated navigation equipment (GPS device) is assumed to be present. The vehicle is able to receive traffic state information and store a digital representation of the urban traffic network, as well as experienced travel times and expected travel times for available regional routes.
- We assume that each departing vehicle can receive real-time pre-trip information in the form of prescribed routes, which are dependent on prevailing or future traffic conditions, in 10-s intervals.
- We assume that each driver completely follows the route prescribed to them, selected from the alternative κ-shortest routes provided at their origin region.
- For every origin-destination pair, public transit is available with capacity large enough so that travel times can be considered constant.
- We make use of a predictive routing method, in this case Incremental Route Planning (IRP), to represent the 1st class of travelers.
- We make use of a non-predictive routing method, in this case Proxy Regret Matching (PRM), to represent the compliant segment

of 2nd traveler class drivers.
- We make use of Multinomial Logit Routing (MLR) to represent the non-compliant segment of 2nd class travelers drivers, as well as the 3rd class travelers.
- Regarding the forecasting step of our predictive routing method, when applied simultaneously with other methods, we consider two scenarios. In the first scenario (S1), we assume that the 1st traveler class make use of privately-owned autonomous vehicles. The information regarding the routes taken from travelers belonging to the 2nd and 3rd classes is unavailable to them. In the second scenario (S2), we assume that the 1st class travelers use a one-way, ride-sharing service, which employs publicly-owned autonomous vehicles. The information regarding the routes taken from 2nd to 3rd class travelers is assumed to be provided to them from the transportation authority in the form of historical or real-time data, or a fusion thereof.

Concretely, in (S1), starting from the beginning of the forecasting simulation, we assign trips based on Multinomial Logit Routing to all departed vehicles, which are not using our predictive routing method. Thus, our forecasting step takes into consideration the fact that the routing approaches used by proprietary route guidance and information systems are unknown and can only be modeled by MLR. Scenario (S2) is modeled during the forecasting step as 1st traveler class possessing complete information regarding the 2nd and 3rd class travelers' route choices up until the current time step. Public transportation service employing autonomous vehicles in a similar manner to (S2) is already undergoing trials in the city-state of Singapore (Illmer, 2016).

The aforementioned assumptions are considered to hold for large metropolitan areas and are expected to be commonplace for most urban areas in the near future. As justification regarding our selection of routing method for each traveler class, we make the following arguments.

(a) We make use of a non-predictive routing method, based on strategic learning, to represent the compliant segment of 2nd traveler class drivers, so as to account for the type of route guidance and information systems currently in use by the majority of human-driven vehicles. We assume that consumer inertia will ensure that this type of guidance will still be employed on metropolitan areas, at least in the foreseeable future.
(b) We make use of a predictive routing method, which employs simulation-based forecasting, to represent the 1st class of travelers, so as to account for the type of route guidance and information systems expected to be installed on autonomous vehicles.
(c) Finally, we make use of multinomial logit routing to represent the non-compliant segment of 2nd class travelers, as well as the 3rd class travelers, which we assume select their routes based on individual preference and past experience, since their route travel time perception is imperfect.

3.5. Network performance benchmarks

We now define several performance metrics by which we will try to compare the effects of each region-based routing method on the regional network performance:

- $\mathscr{C}_{\mathrm{TVT}} = T_s \sum_{h=1}^{H} \sum_{i \in \mathscr{K}} \left(\sum_{z \in \mathscr{Z}_i} \lambda_z \Lambda_z n_i(h) \right)$, the Total Vehicle Travel time for all regions
- $\mathscr{C}_{\mathrm{v}^2} = \sum_{h=1}^{H} \sum_{i,j \in \mathscr{K}} (v_i(n_i(h)) - v_j(n_j(h)))^2$ the sum of squares of average regional speed variabilities for all regions
- $\mathscr{C}_{\mathrm{PTD}}$, Public Transit Diversion, i.e., the fraction of total demand generated throughout the simulation, which is diverted to Public Transit
- $\mathscr{C}_{\mathrm{ITR}}$, Incomplete Trips Rate, i.e., the fraction of total demand generated throughout the simulation, which has not completed their trips by the end of the simulation
- $\mathscr{C}_{\mathrm{ATT}}$, the Average Traveling Time for each traveler on the regional urban network

The total vehicle travel time can be found using the total number of vehicles arriving at the region over a defined time interval T_s. The speed variability metric measures how evenly traffic load is distributed and, implicitly, demonstrates the phenomenon of build up of congestion to capacity in some regions, while other regions receive very little traffic. The performance metric $\mathscr{C}_{\mathrm{PTD}}$ represents the number of potential travelers unable to utilize the urban network, as a fraction of the number of vehicle requests from all origins to all destinations throughout the simulation horizon. Since the speed selected for public transit is lower than the average speed corresponding to the critical accumulation value, this metric is able to demonstrate indirectly the aggregate cost of network underutilization due to overcritical congestion levels. The Incomplete Trips Rate $\mathscr{C}_{\mathrm{ITR}}$ implicitly showcases the network throughput performance. Finally, the Average Traveling Time $\mathscr{C}_{\mathrm{ATT}}$ is calculated as the weighted average of total travel time for all vehicles and provides an easily quantifiable measure of individual traveler benefits obtained through the introduction of autonomous (1st class) and RGIS-equipped (2nd class) vehicles.

4. Simulation results

A diamond-shaped grid network is considered for implementation of our extension of the NTM. The network consists of 16 regions, with an area of 25 km^2 (5×5) for each region, as shown in Fig. 3. It should be noted that, as the focus of this paper is on the interaction of varied routing methods, we have opted for a less sophisticated network test case, where the Urban-scale MFDs for all regions are identical.

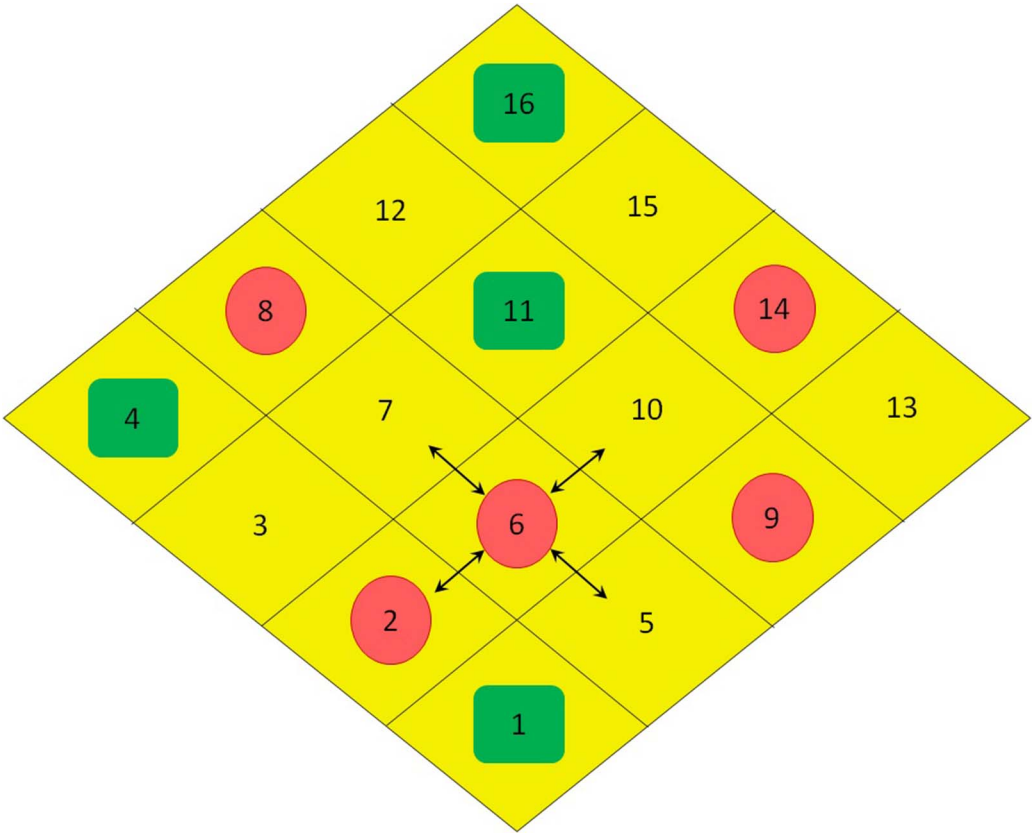

Fig. 3. Layout of the 4 × 4 regional network, where green squares and red circles denote origins and destinations, respectively. (For interpretation of the references to colour in this figure legend, the reader is referred to the web version of this article.)

The homogeneous regions are each described by an Urban-scale MFD with critical accumulation $n_{i,crit} = 25$ veh/km, region network length $\sum_{z\in\mathscr{R}_i} \lambda_z \Lambda_z = 10$ km and free flow speed $v_{i,f} = 45$ km/h, $\forall\, i \in \mathscr{K}$. Capacity along the boundaries is $c_{i,j} = 2000$ veh/h/lane, $\forall\, i,j \in \mathscr{K}, (i,j) \in \mathscr{A}$. For each region i, all regions j such that $(i,j) \in \mathscr{A}$ are defined as the ones that are in the northwest-southeast or northeast-southwest directions with respect to the location of the region i. The demand (veh/h) for each origin-destination pair is shown in Table 1. We introduce disturbance to the demand through time-varying factor multiplication to increase the level of realism of our simulations. At each time step, the demand values are multiplied by a uniformly distributed random number with mean value 1 and variance 0.1. The simulation horizon $H = 2$ h 30 min or 9000 s. The sample time $T_s = 10$ s. It should be noted, that in our case, we use prescriptive route guidance with pre-trip information dissemination. This means that, contrary to the case of en-route guidance, the drivers are not the ones updated, rather, the origin regions are updated regarding the traffic conditions every 10 s and drivers at the current departure time h are assigned the corresponding updated routes. For the 2nd class of travelers using Proxy Regret Matching routing, we test for non-compliance rates $NC \in \{0\%,50\%,70\%\}$. These values might be viewed as appropriately chosen, given that in previous studies, non-compliance rates were shown to be dependent on expected travel time reliability and at the aggregate level, travel time estimation is expected to be less accurate than at the individual link route guidance case. We assume that threshold coefficient $r_{IRP} = 1.0$ for the Public Transit Diversion mechanism in IRP (Incremental Route Planning) routing and similarly $r_{PRM} = 1.0$ for PRM (Proxy Regret Matching) routing. We ran 10 replications for each routing approach and took the average of each respective performance metric.

Table 1
Origin destination demand matrix.

Origin	Demands (veh/h) Destination			
	Region 2	Region 8	Region 9	Region 14
Region 1	400	720	700	1200
Region 4	760	560	400	560
Region 11	680	480	520	520
Region 16	800	400	400	720

Table 2
Comparison of network performance for each routing method when it is applied to the entire network individually, i.e. MPR = 100%.

MPR = 100%	C_{TVT} (veh·s)	C_{v^2} (km²/h²)	C_{PTD} (%)	C_{ITR} (%)	C_{ATT} (s)
IRP	1.410e+08	1.189e+06	18.44	0.01	1565.2
PRM	1.744e+08	6.603e+06	33.08	10.24	2359.9
MLR	2.428e+08	1.187e+07	26.20	27.60	2972.4

4.1. Results for application of each individual route guidance approach

We compare each routing method when it is applied to the entire network individually. That would mean all travelers use the same routing approach, or in market penetration scheme terms, MPR = 100%. We also introduce alternate rates $MPR \in \{10\%,30\%,50\%,70\%,90\%\}$, to showcase the performance robustness of the predictive and non-predictive routing approaches, when compared to MLR (Multinomial Logit Routing), which we designate as our realistic route choice model for self-interested travelers with imperfect information, i.e. unreliable travel time estimation. Assuming that MPR of the vehicle population employ IRP or PRM, while $(100\%-MPR)$ employ MLR, representing vehicles which are not equipped with RGIS (Route Guidance and Information Systems). The following Table 2 presents performance metric results for IRP, PRM and MLR routing methods integrated with Public Transit Diversion, each with a market penetration rate MPR = 100%:

As is evident from the results from Table 2, IRP outperforms all other routing methods. This, of course, is to be expected, since IRP belongs to the predictive routing approach category, which means that travel time estimation accuracy is the highest amongst all methods compared. PRM finds itself in the middle, performing better than MLR in most metrics, but worse than IRP with respect to all metrics. This result is also consistent with our expectations, since PRM belongs to non-predictive routing approach category, meaning that travel time estimation accuracy is worse than it would be for any predictive routing approach. As expected, the worst performing routing method, when individually applied to the regional network, i.e. the respective market penetration rate MPR = 100%, is the MLR routing method. MLR under-performs in all performance metrics except for the Public Transit Diversion metric C_{PTD}. This has to do with the stochastic nature of the Public Transit Diversion Mechanism for MLR, which is simply represented by an alternate route choice with constant travel time for each corresponding Origin-Destination pair.

Even if we compare to the performance of IRP and PRM with varying degrees of market penetration, we observe that the MLR still performs the worst in the majority of performance metrics, compared to the implementations of IRP and PRM with the lowest market penetration rates (10%). This is to be expected, since MLR travelers' behavior is characterized by self-interest, as well as imperfect travel time information provision. More specifically, from Table 3 we can observe that for all combinations of market penetration rates $MPR_{IRP} \setminus MPR_{MLR}$, (S2) scenario results are better than the respective results for scenario (S1). That is to be expected, since the information provided during (S2) is considered to be perfect, when it comes to the route choices of travelers not employing IRP and subsequently, the travel time estimation accuracy is higher. Finally, from Table 4 we can see that IRP performs consistently better than PRM, for respective market penetration rate combinations. Even for $MPR_{IRP} \setminus MPR_{MLR} = 30\% \setminus 70\%$ for both (S1), (S2), we can see that most performance metric results are better than for PRM with a market penetration rate $MPR_{PRM} = 100\%$.

Based on the results from Tables 2–4, we decided to use MLR as our reference routing method and measure the performance gains of IRP, for scenarios (S1), (S2), as well as PRM for various non-compliance rates $NC \in \{0\%,50\%,70\%\}$. The performance metric we derive for said comparison is described in Eq. (17) as the weighted average of all performance metric ratios.

Table 3
IRP (Incremental Route Planning) routing for various MPR (Market Penetration Rates) and for scenarios (S1), (S2).

Scenario	(S1)				
$MPR_{IRP} \setminus MPR_{MLR}$(%\%)	90\10	70\30	50\50	30\70	10\90
C_{TVT} (veh·s)	1.445e+08	1.447e+08	1.545e+08	1.812e+08	2.146e+08
C_{v^2} (km²/h²)	1.208e+06	1.144e+06	1.698e+06	5.258e+06	9.742e+06
C_{PTD} (%)	17.35	15.32	13.28	18.46	26.01
C_{ITR} (%)	0.10	0.01	0.87	6.34	17.68
C_{ATT} (s)	1584.1	1549.1	1605.6	1949.0	2566.2
Scenario	(S2)				
$MPR_{IRP} \setminus MPR_{MLR}$(%\%)	90\10	70\30	50\50	30\70	10\90
C_{TVT} (veh·s)	1.435e+08	1.450e+08	1.529e+08	1.768e+08	2.131e+08
C_{v^2} (km²/h²)	1.191e+06	1.156e+06	1.289e+06	4.674e+06	9.654e+06
C_{PTD} (%)	17.38	15.47	13.07	17.24	25.61
C_{ITR} (%)	0.05	0.0	0.0	5.30	18.15
C_{ATT} (s)	1574.0	1553.1	1587.3	1870.2	2527.6

Table 4
PRM (Proxy Regret Matching) routing with for various MPR (Market Penetration Rates) assuming that NC = 0% non-compliance rate.

Non-compliance	NC = 0%				
$MPR_{PRM} \backslash MPR_{MLR}(\%\backslash\%)$	90\10	70\30	50\50	30\70	10\90
C_{TVT} (veh·s)	1.729e+08	1.768e+08	1.825e+08	2.001e+08	2.239e+08
C_{v^2} (km^2/h^2)	6.223e+06	6.505e+06	7.555e+06	9.189e+06	1.106e+07
C_{PTD} (%)	31.98	32.26	31.04	30.53	30.91
C_{ITR} (%)	9.01	5.36	5.78	9.68	19.93
C_{ATT} (s)	2302.9	2369.6	2383.0	2597.7	2914.0

$$\mathscr{C}_{\mathrm{RWA}} = \frac{\left\{ w_{TVT} \frac{\mathscr{C}_{\mathrm{TVT,g}}}{\mathscr{C}_{\mathrm{TVT,MLR}}} + w_v \frac{\mathscr{C}_{\mathrm{v,g}}}{\mathscr{C}_{\mathrm{v,MLR}}} + w_{PTD} \frac{\mathscr{C}_{\mathrm{PTD,g}}}{\mathscr{C}_{\mathrm{PTD,MLR}}} + w_{ITR} \frac{(1-\mathscr{C}_{\mathrm{ITR,MLR}})}{(1-\mathscr{C}_{\mathrm{ITR,g}})} + w_{ATT} \frac{\mathscr{C}_{\mathrm{ATT,g}}}{\mathscr{C}_{\mathrm{ATT,MLR}}} \right\}}{(w_{TVT} + w_v + w_{PTD} + w_{ITR} + w_{ATT})} \tag{17}$$

where $g \in \{IRP(S1), IRP(S2), PRM(NC), IRP(S1) \backslash PRM(NC) \backslash MLR, IRP(S2) \backslash PRM(NC) \backslash MLR\}$ and $W = \{w_{TVT}, w_v, w_{PTD}, w_{ITR}, w_{ATT}\}$ a set of appropriate weights to denote the importance we place on the respective performance measures. In our test case, all weights are set to $w_{TVT} = w_v = w_{PTD} = w_{ITR} = w_{ATT} = 1$.

After we calculate the $\mathscr{C}_{\mathrm{RWA}}$ values for all routing methods other than MLR, we can derive the Performance gain – Market Penetration curves for non-predictive routing method PRM, as well as predictive routing methods IRP (S1) and IRP (S2), see Fig. 4. We can easily observe that, for IRP, overall network performance exceeds that of PRM in all corresponding degrees of market penetration. Performance gains of PRM seem to increase with MPR values up to 90%. When MPR = 100%, there is a 2.2%

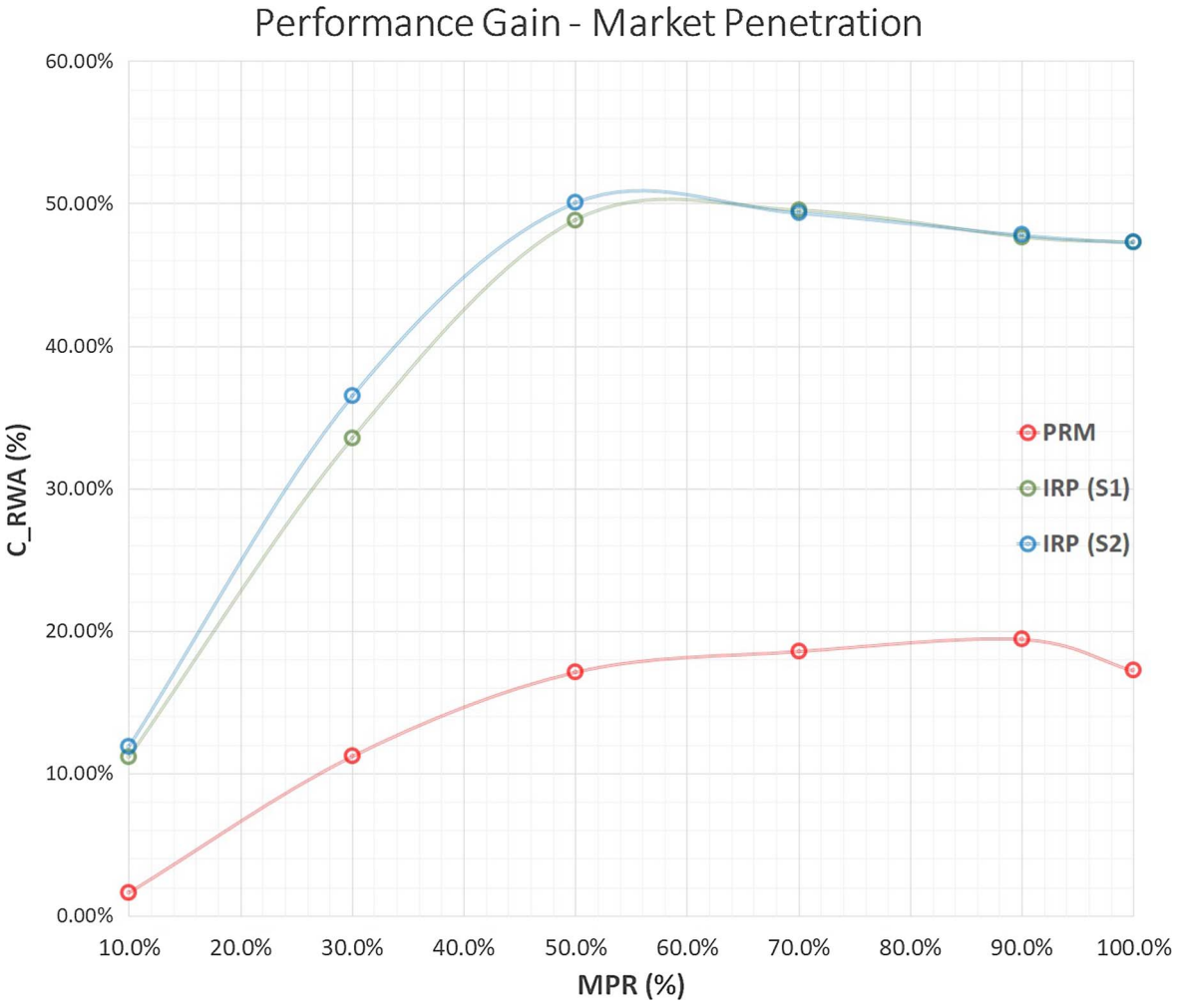

Fig. 4. Performance gain – Market penetration curves of PRM, IRP (S1), IRP (S2), for penetration rates $MPR \in \{10\%,30\%,50\%,70\%,90\%\}$.

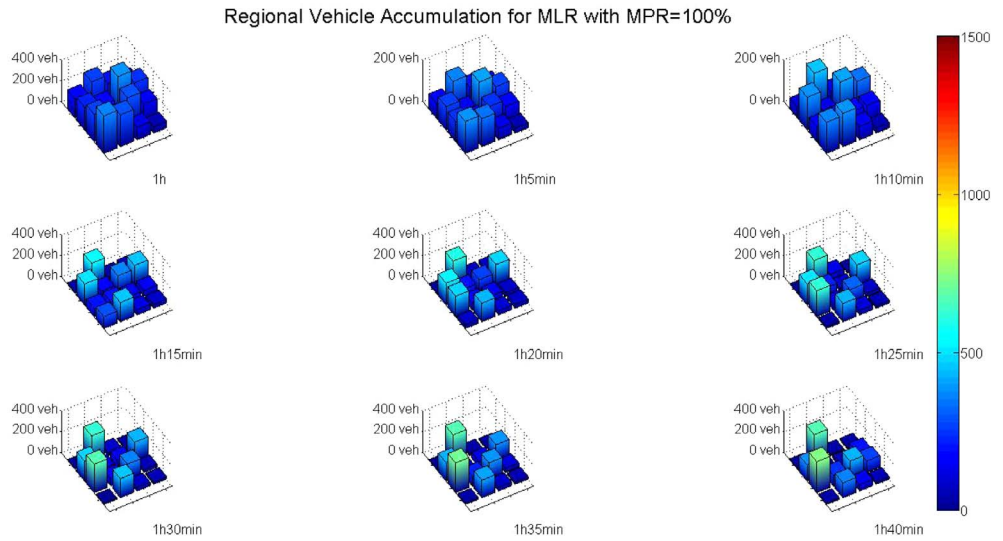

Fig. 5. Vehicle accumulation for MLR from 1 h to 1 h 40 min of the simulation, at 5 min intervals, in regions 1–16.

performance loss compared to MPR = 90%. This can be attributed to the fact, while PRM at various degrees of market penetration will improve overall network performance, having a percentage of self-interested travelers using MLR, allows for higher network resource utilization. In the case of MLR, all available routes will be used with some probability, however small, and never zero, thus distributing demand along alternative routes that might not have been considered by PRM. We can also observe that for PRM, the weighted average values of $\mathscr{C}_{\mathrm{ITR}}$ peak at MPR = 70%. From our results for individual routing method performance, which have been omitted for brevity, as the MPR for PRM increases, the individual ITR values for PRM also increase, while we observe the simultaneous converse effect for travelers using MLR. So MPR = 70% could be described as the intersection of the increasing ITR values for PRM and decreasing ITR values for MLR. In the case of scenarios (S1), (S2) for IRP, performance gains seem to increase in tandem with the degree of market penetration, however we see that for MPR $\geqslant$ 50%, performance gradually decreases until, at MPR = 100%, it reaches a value of $\mathscr{C}_{\mathrm{RWA}} \approx 47\%$ which lies in between values achieved for MPR = 50% ($\mathscr{C}_{\mathrm{RWA}} \approx 50\%$) and MPR = 30% ($\mathscr{C}_{\mathrm{RWA}} \approx 35\%$). These results demonstrate that performance gains are dependent on the forecasting step methodology we follow. While higher degrees of market penetration are required for better overall network performance, the virtual vehicle generation and route assignment leads to less accurate travel time prediction, owing to the fact that we employ MLR for virtual vehicle route assignment. Therefore, having fewer unequipped vehicles as part of the vehicle population leads to diminishing performance gains. Nevertheless, performance robustness for both IRP (S1) and IRP (S2) is assured, as is evident from the consistent gain in performance for every degree of market penetration.

Figs. 5–7 show vehicle accumulation levels per region starting from 1 h (3600 s) of the simulation up until 1 h 40 min (6000 s) with 5 min intervals, for 100% market penetration for each routing method (MLR, PRM, IRP) with region numbering as in Fig. 3. This particular simulation time period was selected because it contains the simulation midpoint and the effect each routing method has, is easy to discern.

As is evident from Figs. 5–7, during these 40 min of simulation, IRP manages to keep vehicle accumulation levels below 500 veh. for all regions, in addition to maintaining a more even distribution of vehicles over all regions. PRM is able to maintain vehicle accumulation levels below 500 vehicles for 14 out of 16 regions, however the vehicle distribution is not even throughout the regional network. As is expected, MLR is not able to maintain vehicle accumulation levels below 500 veh. for 5 out of 16 regions, while the vehicle distribution over all regions is markedly uneven, compared to IRP and PRM. Based on our network setup, regional vehicle accumulation levels over 500 veh. indicate that regions are congested. Vehicle distribution is an important indicator of network resource utilization. Homogeneous vehicle distribution over all regions signifies higher network resource utilization.

4.2. Comparison of route guidance approaches in mixed class application with various combinations of market penetration rates

We have several mixed class application cases with different combinations of market penetration rates, MPR1 and MPR2, for 1st and 2nd traveler classes respectively. For the prescriptive, pre-trip route guidance provided to the 2nd class of travelers, we extend the compliance model originally suggested by Papageorgiou (1990) whereby a certain fraction of 2nd class travelers will comply to the advice provided and the remaining fraction will disregard it. Concretely, assuming non-compliance rate NC for the 2nd class of travelers, we can say that the travel demand for each traveler class at departure time h for every origin-destination pair, $\forall\, b \in \mathscr{K}_o, e \in \mathscr{K}_d$ is:

$$\zeta_{b,e}^{IRP}(h) = MPR1 \cdot \zeta_{b,e}(h) \tag{18}$$

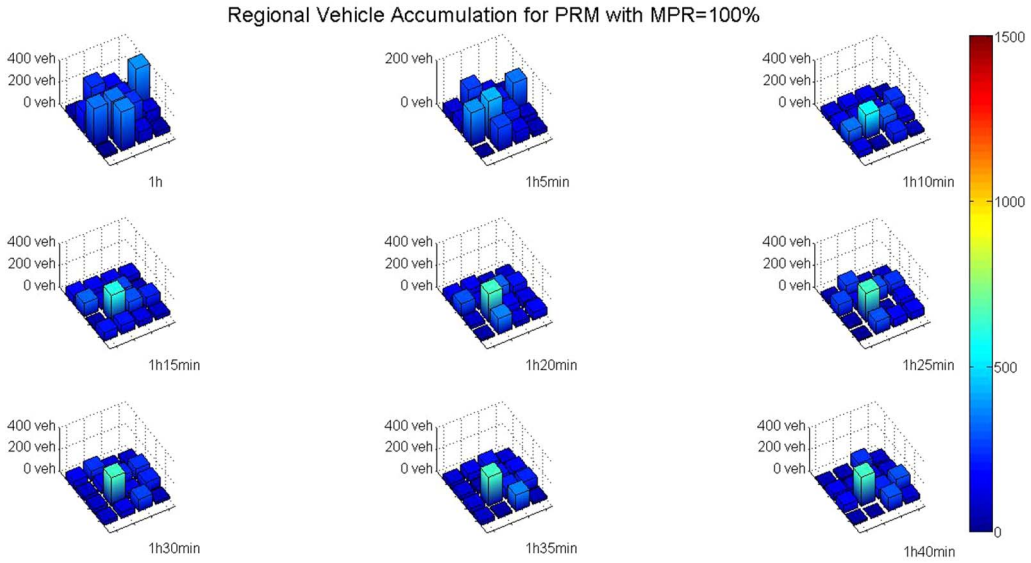

Fig. 6. Vehicle accumulation for PRM from 1 h to 1 h 40 min of the simulation, at 5 min intervals, in regions 1–16.

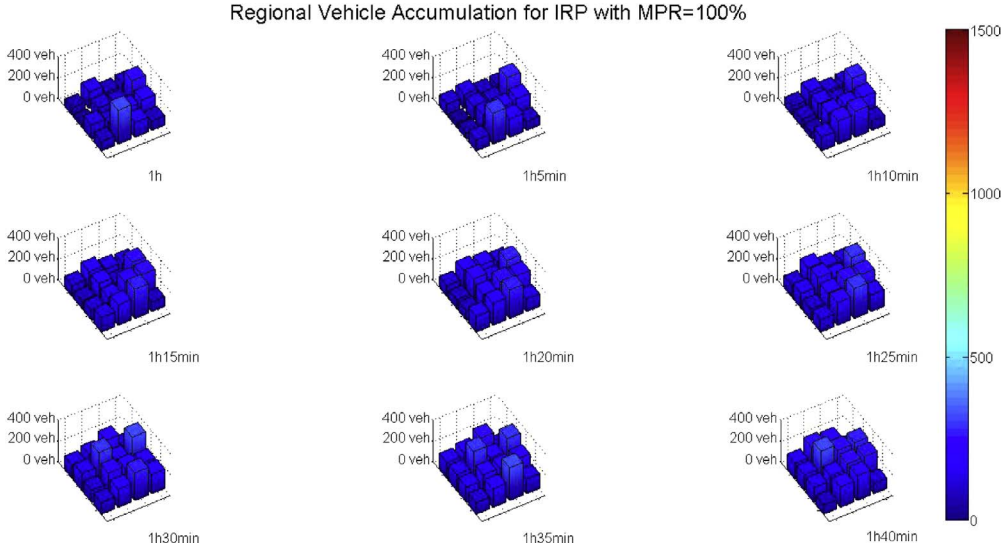

Fig. 7. Vehicle accumulation for IRP from 1 h to 1 h 40 min of the simulation, at 5 min intervals, in regions 1–16.

$$\zeta_{b,e}^{PRM}(h) = (MPR2{-}NC)\cdot\zeta_{b,e}(h) \tag{19}$$

$$\zeta_{b,e}^{MLR}(h) = (1{-}(MPR1 + (MPR2{-}NC))\cdot\zeta_{b,e}(h) \tag{20}$$

We selected 3 market penetration rates which seem consistent with experts' predictions regarding the adoption of autonomous vehicle technology (IEEE, 2012). If we make an approximate backwards extrapolation, we can assume MPR1 = 70% by early 2040, MPR1 = 40% by early 2030 and MPR1 = 10% by early 2020. The market penetration values of 2nd traveler class MPR2 in each mixed class routing scenario are MPR2 = ϕ_{10},ϕ_{10} ∈ {10%,40%,70%}, for MPR1 = 10%, MPR2 = ϕ_{40},ϕ_{40} ∈ {40%,60%}, for MPR1 = 40% and MPR2 = ϕ_{70} = 30%, for MPR1 = 70%. Obviously, in the last 2 scenarios, for ϕ_{40} = 60% and ϕ_{70} = 30%, we assume that the 2nd traveler class comprises the maximum possible percentage such that MPR1 + MPR2 = 100%. We also test for equal market penetration rates MPR1 = MPR2 = MPR3 = 33.3%, so as to more accurately evaluate the overall network performance, when the degree of penetration does not affect the result. For the 2nd class of travelers, we test for non-compliance rates NC ∈ {0%,50%,70%}. As before, we assume that threshold coefficient r_{IRP} = 1 for the Public Transit Diversion mechanism in IRP routing methods and r_{PRM} = 1 for PRM routing method. Similar to Figs. 5–7, Fig. 8 demonstrates regional vehicle accumulation levels for a mixed application of IRP, PRM and MLR with equal market penetration rates MPR1 = MPR2 = MPR3 = 33.3%, during the same simulation time period of 40 min as mentioned before. Table 5 presents individual performance metric results for each routing method in a mixed application of

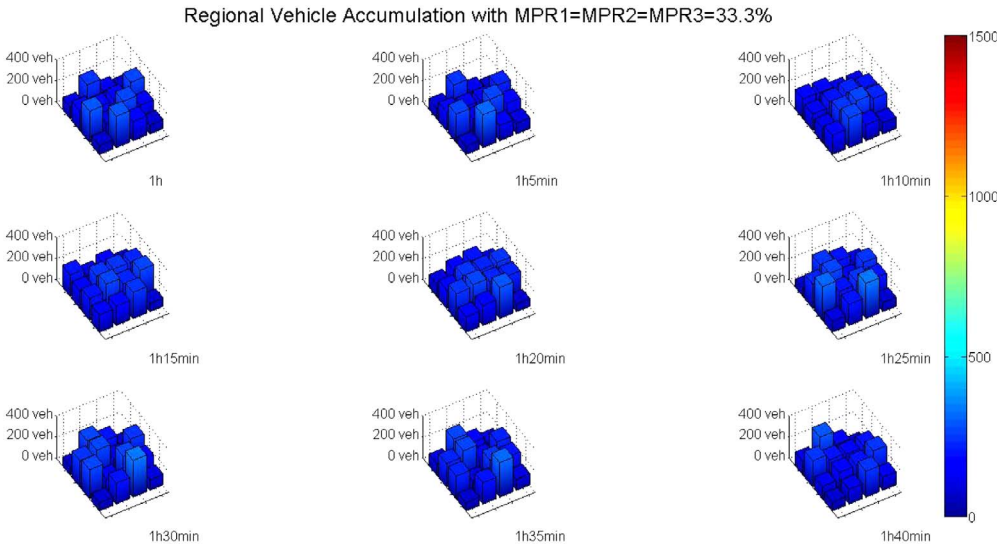

Fig. 8. Regional vehicle accumulation for IRP\PRM\MLR from 1 h to 1 h 40 min of the simulation, at 5 min intervals.

IRP, PRM and MLR with equal market penetration rates MPR1 = MPR2 = MPR3 = 33.3% for non-compliance rates $NC \in \{0\%,50\%,70\%\}$ and scenarios (S1), (S2). Similar to earlier, we selected this market penetration rate combination so as to rate the individual performance of each routing method, where the degree of penetration plays no role for the results, but PRM's non-compliance rate is also evaluated. Table 6 presents individual performance metric results for each routing method in a mixed application of IRP, PRM and MLR with market penetration rates MPR1 = MPR2 = 10% and MPR3 = 80% for non-compliance rates $NC \in \{0\%,50\%,70\%\}$ and scenarios (S1), (S2). We selected this particular market penetration rate combination to demonstrate the value of IRP in a mixed class application setting with very low market penetration for both 1st and 2nd class travelers. Table 7 presents performance gain results for all market penetration rate and non-compliance rate combinations mentioned above for mixed application of IRP (S1), IRP (S2), PRM (NC) and MLR. It should be noted that, due to space considerations, we will focus our individual performance metric results analysis on the case of equivalent market penetration rates as well as the case where MPR1 and MPR2 are the lowest market penetration rates in a mixed class application setting. More specifically, MPR1 = MPR2 = 10% and MPR3 = 80%. It should be stated that individual performance metric results are used to derive all the performance gain results as presented in Table 7.

As is evident from Fig. 8, regional vehicle accumulation levels never exceed 500 veh., however, compared to an application of IRP with MPR = 100%, as seen in Fig. 7, vehicle distribution over all regions appears to be more uneven. As a general observation from Table 7, we can see that for most market penetration rates for (S2) and when MPR1 = 40% for (S1), when non-compliance rate NC is higher, performance is the highest. This can be attributed to the fact, that, during the forecasting step of IRP, all virtual vehicles

Table 5
Comparison of individual performance metrics for each routing method when it is for a mixed application of IRP, PRM and MLR with equal market penetration rates MPR1 = 33.3%, MPR2 = 33.3(1 − NC)%, MPR3 = 33.3(1 + NC)% with NC = 0%, 50%, 70% for scenarios (S1), (S2).

MPR1 = 33.3%, MPR2 = 33.3(1 − NC)%, MPR3 = 33.3(1 + NC)%						
Scenario	(S1)			(S2)		
	C_{PTD} (%)	C_{ITR} (%)	C_{ATT} (s)	C_{PTD} (%)	C_{ITR} (%)	C_{ATT} (s)
NC = 0%						
IRP	39.99	0.62	1504.5	28.26	0.0	1479.3
PRM	24.60	0.09	1876.8	27.48	0.14	1792.4
MLR	0.90	1.17	1713.9	0.09	0.0	1614.4
NC = 50%						
IRP	42.73	0.14	1432.9	32.79	0.05	1493.9
PRM	24.89	0.22	1831.8	28.61	0.14	1826.7
MLR	0.51	0.55	1662.6	0.31	0.59	1660.9
NC = 70%						
IRP	38.11	0.99	1558.9	35.36	0.02	1499.6
PRM	25.35	0.34	1915.3	29.00	0.12	1869.6
MLR	0.89	2.79	1801.8	0.51	0.40	1705.6

Table 6
Comparison of individual performance metrics for each routing method when it is for a mixed application of IRP, PRM and MLR with market penetration rates MPR1 = 10%, MPR2 = 10(1 − NC)%, MPR3 = (80 + 10NC)% with NC = 0%, 50%, 70% for scenarios (S1), (S2).

MPR1 = 10%, MPR2 = 10(1 − NC)%, MPR3 = (80 + 10NC)%						
Scenario	(S1)			(S2)		
	C_{PTD} (%)	C_{ITR} (%)	C_{ATT} (s)	C_{PTD} (%)	C_{ITR} (%)	C_{ATT} (s)
NC = 0%						
IRP	49.77	0.45	1284.7	57.94	0.42	1589.1
PRM	57.10	0.19	1022.2	48.43	0.84	2349.0
MLR	28.25	8.72	1584.3	17.75	17.20	2519.6
NC = 50%						
IRP	61.55	0.49	1073.1	61.22	0.04	1447.3
PRM	50.88	0.20	1175.4	49.55	0.42	2387.7
MLR	27.95	8.29	1443.0	19.14	19.68	2567.0
NC = 70%						
IRP	59.17	0.32	1595.4	60.78	0.07	1491.5
PRM	50.49	0.27	2454.7	51.58	0.24	2376.3
MLR	20.08	19.07	2580.0	19.60	19.42	2575.8

Table 7
Various market penetration rate combinations for scenarios (S1), (S2) of IRP representing 1st class travelers, PRM representing 2nd class travelers with NC = 0%, 50%, 70% non-compliance rate and MLR representing non-compliant segment of 2nd class, as well as 3rd class travelers.

Ratio weighted average	C_{RWA}(%)					
Scenarios	(S1)			(S2)		
MPR1\MPR2\MPR3 for IRP\PRM\MLR (%\%\%)	NC(%)					
	0	50	70	0	50	70
10\10(1 − NC)\(80 + 10·NC)	9.74	15.96	13.60	15.80	14.44	14.39
10\40(1 − NC)\(50 + 40·NC)	27.64	18.62	15.66	28.70	20.25	17.84
10\70(1 − NC)\(20 + 70·NC)	27.02	28.42	19.92	30.13	28.30	20.31
33.3\33.3(1 − NC)\33.3(1 + NC)	40.73	45.34	42.97	46.25	47.35	46.85
40\40(1 − NC)\(20 + 40·NC)	42.30	47.80	48.81	46.38	48.53	49.82
40\60(1 − NC)\60·NC	36.12	44.19	48.85	43.73	47.36	48.87
70\30(1 − NC)\30·NC	44.51	48.31	48.14	46.81	48.37	48.51

generated from the current step *h* onwards, are assigned a route choice based on MLR. High NC values mean that more travelers not belonging to 1st class, are assigned routes based on MLR rather than PRM, improving travel time estimation accuracy for IRP during the mixed class application. This also means that PRM does not contribute as much as IRP to the overall network performance. Another observation is that when MPR1 > 30%, performance gains compared to MLR for when $MPR_{MLR} = 100\%$, the worst-performing routing method, almost always exceed 40%, for all non-compliance rate combinations. Even for MPR1\MPR2\MPR3 = 10%\10%\80%, with NC = 70%, the case with least market penetration for both IRP and PRM, for the more realistic scenario (S1), we can still see a performance gain of 13.60%. IRP for (S1), in combination with PRM, can potentially benefit overall network performance, provided that 50% ⩾ NC ⩽ 70%, even though MPR1 and MPR2 are as low as 10%. We also demonstrated the positive influence of autonomous vehicles in the overall network performance, evidenced by a performance gain $\mathscr{G}_{\mathrm{RWA}} = 40.73\%$ for (S1) and $\mathscr{G}_{\mathrm{RWA}} = 46.25\%$, given equal market penetration rates MPR1 = MPR2 = MPR3 = 33.3% and non-compliance rate NC = 0%. Individual performance metric results from Tables 5 and 6 provide us with a more detailed insight regarding the different effect the degree of market penetration, as well as the information provided to IRP in scenarios (S1) and (S2) has on Public Transit Diversion, Incomplete Trips Rate and Average Travel Time for each routing method. PTD values for IRP never exceed 45% which is less than the lowest PTD value for IRP for all market penetration rate combinations where MPR3 < 30%.. As expected, the highest PTD rate for IRP is for (S1) with NC = 0% and the lowest PTD rate for IRP is for (S2) with NC = 0%. The reason for this is the fact that in (S1), IRP's forecasting step accuracy is diminished, due to information available only for the 1st class travelers. All other traveler classes are assigned routes based on MLR. On the other hand, for (S2) and NC = 0%, IRP's forecasting step accuracy is higher for this particular combination of market penetration rates, since information is available for both 1st and 3rd traveler classes. Due to it's overall high PTD rate, IRP presents with the lowest ATT in both (S1) and (S2). More specifically, we observe that when the individual PTD rate for IRP exceeds 40%, PTD contributes the most to the reduction of individual ATT for IRP, as is the case for (S1) and NC = 50%. Another positive effect of IRP is the reduction of individual PTD rate for MLR, which drops below 1%. While the ITR for IRP for (S2) tends to be the lowest, for (S1), due to the limited information availability, prediction is not as accurate, leading to ITR

almost half of that for MLR, which exhibits the highest ITR rate for all but one NC/Scenario combinations. The ATT for PRM is consistently lagging behind the ATT for IRP and MLR. The best performing ATT for PRM is for (S2) and NC = 0%. This means that we can indirectly observe the effect market penetration rate has on the individual performance of PRM and MLR, but not IRP, as 1st class travelers are assumed to be fully compliant. ITR for PRM is at it's lowest for (S2), followed closely by (S1). Additionally, one must take into consideration the beneficial effect the 1st traveler class, employing IRP, has on the 2nd and especially the 3rd traveler class. Compared to ATT results for PRM from Tables 2 and 4, for several degrees of penetration, ranges from 18% to 30% improvement on the ATT for PRM in the mixed application. It should be noted that the ATT for MLR seems to benefit the most from the presence of 1st class travelers, as can be seen from the improvement ranging between 40% and 45%, compared to results from Table 2. Compared to MLR, PRM seems to benefit less from IRP, however, compared to performance results when IRP is absent, see Table 4, there is individual improvement of approximately 10% for ITR and 22% for ATT of PRM. We can observe that, owing to the higher PTD rate values for IRP in all combinations but the one for NC = 0% (S1), ATT for IRP never exceeds 1600 s, whereas ATT for PRM and MLR exceed 2000 s in the majority of combinations. For NC = 0% (S1), ATT for PRM is shorter than ATT for IRP, which can be explained by the fact that this is the only case where the PTD value for PRM is higher than that of IRP. In all combinations, ITR for MLR never goes lower than 8%, whereas ITR values for IRP and PRM never exceed 0.50% and 0.90% respectively. While this could be partly attributed to IRP's and PRM's superior performance, the main factor is the comparatively low degree of market penetration both for 1st and 2nd traveler classes, employing IRP and PRM respectively.

5. Conclusions and future research

In this paper, we have introduced a multi-class extension of the Network Transmission Model, used to simulate regional traffic dynamics. We presented three types of region-based routing approaches, an innovative predictive routing method with Public Transit Diversion called IRP (Incremental Route Planning), a non-predictive routing method with Public Transit Diversion integration called PRM (Proxy Regret Matching), as well as an extension of MLR (Multinomial Logit Routing), which also includes Public Transit Diversion. We compared the individual performance of each method, when applied to a regional traffic network. We used IRP to represent a class of travelers which employ autonomous vehicles. We used PRM to represent a class of travelers which employ conventional vehicles equipped with RGIS (Route Guidance and Information Systems). We used MLR to represent a class of travelers which employ unequipped, conventional vehicles. Our main contribution is the investigation of mixed traveler class interaction on a regional traffic network, through mixed application of the IRP, PRM and MLR routing methods. We considered 2 scenarios for the autonomous vehicles, which make use IRP for fully compliant route guidance. In (S1), autonomous vehicles are assumed to be privately owned, which means that information provision is limited to other autonomous vehicles only. Hence, travel time prediction accuracy is negatively affected by the assumption that all other vehicles are routed as if unequipped with RGIS. In (S2), autonomous vehicles are assumed to be publicly owned, as part of a public one-way ridesharing service which means that information provision includes historical and real-time data about all vehicles in the urban traffic network. Hence, travel time prediction accuracy is positively affected. In essence, market penetration rates were varied explicitly through specification of MPR1, MPR2, MPR3 for 1st, 2nd and 3rd traveler class respectively, as well as non-compliance rates NC for 2nd class of travelers. In addition, respective market penetration rates for 1st, 2nd and 3rd traveler classes were varied implicitly through the introduction of Public Transit Diversion mechanisms to each routing method employed to represent each distinct traveler class. We were able to observe performance gains ranging from approximately 10–50%, compared to individual application of MLR, a more realistic reference case. IRP was consistently providing 1st class travelers with the shortest ATT, implicitly guaranteeing full compliance, even in the case full compliance is not a mandatory feature for 1st class travelers. This indicates the positive potential impact of autonomous vehicle technology adoption.

In future work, we aim to add sophistication to our Public Transit Model by introducing passenger transition delays and train frequency, with varying travel times. We also aim to introduce a more sophisticated compliance model, so that 2nd class traveler compliance is dependent on the travelers' travel time information reliability, as well as their level of familiarity with the route assigned to them. Based on our current results regarding ATT for PRM in a mixed-class application setting, one could argue that 2nd class travelers would become non-compliant, eventually being subsumed by the 3rd traveler class. Our aim is to introduce congestion pricing as an additional traffic management measure, where departure time can be considered as an additional decision variable, so that we can eliminate the difference in individual performance between PRM and MLR, thus reaching a stable market penetration rate combination. In addition, we shall investigate the interaction of multiple types of routing methods with congestion pricing and make observations on the overall network performance.

References

Aboudolas, K., Geroliminis, N., 2013. Perimeter and boundary flow control in multi-reservoir heterogeneous networks. Transport. Res. Part B: Methodol. 55, 265–281.
Aboudolas, K., Papageorgiou, M., Kosmatopoulos, E., 2009. Store-and-forward based methods for the signal control problem in large-scale congested urban road networks. Transport. Res. Part C: Emerg. Technol. 17, 163–174.
Adler, J.L., Satapathy, G., Manikonda, V., Bowles, B., Blue, V.J., 2005. A multi-agent approach to cooperative traffic management and route guidance. Transport. Res. Part B: Methodol. 39, 297–318.
Ampountolas, K., Zheng, N., Geroliminis, N., 2014. Perimeter flow control for bi-modal urban road networks. In: Transportation Research Board 93rd Annual Meeting.
de Cea Ch, J., Valverde, G.G., et al., 2009. Effect of advanced traveler information systems and road pricing in a network with non-recurrent congestion. Transport. Res. Part A: Policy Pract. 43, 481–499.
Chen, O., Ben-Akiva, M., 1998. Game-theoretic formulations of interaction between dynamic traffic control and dynamic traffic assignment. Transport. Res. Rec.: J. Transport. Res. Board 179–188.

Chiabaut, N., 2015. Evaluation of a multimodal urban arterial: the passenger macroscopic fundamental diagram. Transport. Res. Part B: Methodol. 81, 410–420.
Daganzo, C.F., 1994. The cell transmission model: a dynamic representation of highway traffic consistent with the hydrodynamic theory. Transport. Res. Part B: Methodol. 28, 269–287.
Daganzo, C.F., 2007. Urban gridlock: macroscopic modeling and mitigation approaches. Transport. Res. Part B: Methodol. 41, 49–62.
Daganzo, C.F., Gayah, V.V., Gonzales, E.J., 2011. Macroscopic relations of urban traffic variables: bifurcations, multivaluedness and instability. Transport. Res. Part B: Methodol. 45, 278–288.
Dingus, T.A., Guo, F., Lee, S., Antin, J.F., Perez, M., Buchanan-King, M., Hankey, J., 2016. Driver crash risk factors and prevalence evaluation using naturalistic driving data. Proc. Nat. Acad. Sci. 113, 2636–2641.
Dixit, V.V., Radwan, E.A., Board, T.R., 2007. Strategies to improve dissipation into destination networks using macroscopic network flow models. Fundam. Diagr. Traffic Flow Theory 212.
Drake, J., Schoffer, J., May, A., 1967. A statistical analysis of speed density hypothesis. Highway Res. Rec. 154.
van Essen, M., Thomas, T., van Berkum, E., Chorus, C., 2016. From user equilibrium to system optimum: a literature review on the role of travel information, bounded rationality and non-selfish behaviour at the network and individual levels. Transport Rev. 36, 527–548.
Etemadnia, H., Abdelghany, K., Hassan, A., 2014. A network partitioning methodology for distributed traffic management applications. Transportmet. A: Transport Sci. 10, 518–532.
Fagnant, D.J., Kockelman, K.M., 2014. The travel and environmental implications of shared autonomous vehicles, using agent-based model scenarios. Transport. Res. Part C: Emerg. Technol. 40, 1–13.
Ford, D.R., Fulkerson, D.R., 1962. Flows in Networks. Princeton University Press, Princeton, NJ, USA.
Garcia, A., Reaume, D., Smith, R.L., 2000. Fictitious play for finding system optimal routings in dynamic traffic networks. Transport. Res. Part B: Methodol. 34, 147–156.
Gayah, V.V., Gao, X.S., Nagle, A.S., 2014. On the impacts of locally adaptive signal control on urban network stability and the macroscopic fundamental diagram. Transport. Res. Part B: Methodol. 70, 255–268.
Geroliminis, N., Daganzo, C.F., 2007. Macroscopic modeling of traffic in cities. In: Transportation Research Board 86th Annual Meeting.
Geroliminis, N., Haddad, J., Ramezani, M., 2013. Optimal perimeter control for two urban regions with macroscopic fundamental diagrams: a model predictive approach. IEEE Trans. Intell. Transport. Syst. 14, 348–359.
Geroliminis, N., Levinson, D.M., 2009. Cordon pricing consistent with the physics of overcrowding. In: Transportation and Traffic Theory 2009: Golden Jubilee. Springer, pp. 219–240.
Geroliminis, N., Sun, J., 2011a. Hysteresis phenomena of a macroscopic fundamental diagram in freeway networks. Transport. Res. Part A: Policy Pract. 45, 966–979.
Geroliminis, N., Sun, J., 2011b. Properties of a well-defined macroscopic fundamental diagram for urban traffic. Transport. Res. Part B: Methodol. 45, 605–617.
Geroliminis, N., Zheng, N., Ampountolas, K., 2014. A three-dimensional macroscopic fundamental diagram for mixed bi-modal urban networks. Transport. Res. Part C: Emerg. Technol. 42, 168–181.
Godfrey, J., 1969. The mechanism of a road network. Traffic Eng. Control 8.
Gonzales, E.J., 2015. Coordinated pricing for cars and transit in cities with hypercongestion. Econ. Transport. 4, 64–81.
Haddad, J., Mirkin, B., 2017. Coordinated distributed adaptive perimeter control for large-scale urban road networks. Transport. Res. Part C: Emerg. Technol. 77, 495–515.
Haddad, J., Ramezani, M., Geroliminis, N., 2012. Model predictive perimeter control for two-region urban cities. In: Transportation Research Board 91st Annual Meeting.
Haddad, J., Ramezani, M., Geroliminis, N., 2013. Cooperative traffic control of a mixed network with two urban regions and a freeway. Transport. Res. Part B: Methodol. 54, 17–36.
Haddad, J., Shraiber, A., 2014. Robust perimeter control design for an urban region. Transport. Res. Part B: Methodol. 68, 315–332.
Hajiahmadi, M., Knoop, V.L., De Schutter, B., Hellendoorn, H., 2013. Optimal dynamic route guidance: a model predictive approach using the macroscopic fundamental diagram. In: 2013 16th International IEEE Conference on Intelligent Transportation Systems-(ITSC). IEEE, pp. 1022–1028.
Hart, S., Mas-Colell, A., 2000. A simple adaptive procedure leading to correlated equilibrium. Econometrica 68, 1127–1150.
Herman, R., Ardekani, S., 1984. Characterizing traffic conditions in urban areas. Transport. Sci. 18, 101–140.
Herman, R., Prigogine, I., 1979. A two-fluid approach to town traffic. Science 204, 148–151.
Hoogendoorn, S.P., Bovy, P.H., 1998. Optimal routing control using VMSs. Delft University Press, Delft, The Netherlands.
IEEE, 2012. Ieee news releases, look ma, no hands! URL: <http://www.ieee.org/about/news/2012/5september_2_2012.html> (accessed 20-June-2016).
Illmer, A., 2016. Self-driving Taxi Trial Kicks Off in Singapore. URL: <http://www.bbc.com/news/business-37181956> (accessed 10-September-2016).
Ji, Y., Geroliminis, N., 2012. On the spatial partitioning of urban transportation networks. Transport. Res. Part B: Methodol. 46, 1639–1656.
Ji, Y., Luo, J., Geroliminis, N., 2014. Empirical observations of congestion propagation and dynamic partitioning with probe data for large-scale systems. Transport. Res. Rec.: J. Transport. Res. Board 2422, 1–11.
Jin, W., Zhang, H.M., 2003. On the distribution schemes for determining flows through a merge. Transport. Res. Part B: Methodol. 37, 521–540.
de Jong, D., Knoop, V.L., Hoogendoorn, S.P., 2013. The effect of signal settings on the macroscopic fundamental diagram and its applicability in traffic signal driven perimeter control strategies. In: 2013 16th International IEEE Conference on Intelligent Transportation Systems-(ITSC). IEEE, pp. 1010–1015.
Katrakazas, C., Quddus, M., Chen, W.H., Deka, L., 2015. Real-time motion planning methods for autonomous on-road driving: State-of-the-art and future research directions. Transport. Res. Part C: Emerg. Technol. 60, 416–442.
Kaufman, D.E., Nonis, J., Smith, R.L., 1998. A mixed integer linear programming model for dynamic route guidance. Transport. Res. Part B: Methodol. 32, 431–440.
Keyvan-Ekbatani, M., Gao, X.S., Gayah, V., Knoop, V.L., 2016. Combination of traffic-responsive and gating control in urban networks: Effective interactions. In: Transportation Research Board 95th Annual Meeting.
Keyvan-Ekbatani, M., Kouvelas, A., Papamichail, I., Papageorgiou, M., 2012. Exploiting the fundamental diagram of urban networks for feedback-based gating. Transport. Res. Part B: Methodol. 46, 1393–1403.
Keyvan-Ekbatani, M., Papageorgiou, M., Papamichail, I., 2013. Urban congestion gating control based on reduced operational network fundamental diagrams. Transport. Res. Part C: Emerg. Technol. 33, 74–87.
Keyvan-Ekbatani, M., Yildirimoglu, M., Geroliminis, N., Papageorgiou, M., 2015. Multiple concentric gating traffic control in large-scale urban networks. IEEE Trans. Intell. Transport. Syst. 16, 2141–2154.
Knoop, V., De Jong, D., Hoogendoorn, S., 2014. Influence of road layout on network fundamental diagram. Transport. Res. Rec.: J. Transport. Res. Board 22–30.
Knoop, V., Hoogendoorn, S., Van Lint, J.W., 2012. Routing strategies based on macroscopic fundamental diagram. Transport. Res. Rec.: J. Transport. Res. Board 2315, 1–10.
Knoop, V., Tamminga, G., Leclercq, L., 2016. Network transmission model: application to a real world city. In: Transportation Research Board 95th Annual Meeting.
Knoop, V.L., Hoogendoorn, S.P., 2013. Empirics of a generalized macroscopic fundamental diagram for urban freeways. Transport. Res. Rec.: J. Transport. Res. Board 2391, 133–141.
Knoop, V.L., Hoogendoorn, S.P., 2014. Network transmission model: a dynamic traffic model at network level. In: Transportation Research Board 93rd Annual Meeting.
Knoop, V.L., Hoogendoorn, S.P., 2015. An area-aggregated dynamic traffic simulation model. Eur. J. Transport Infrastruct. Res.(EJTIR) 15 (2), 2015.
Kouvelas, A., Saeedmanesh, M., Geroliminis, N., 2017. Enhancing model-based feedback perimeter control with data-driven online adaptive optimization. Transport. Res. Part B: Methodol. 96, 26–45.
Kuyer, L., Whiteson, S., Bakker, B., Vlassis, N., 2008. Multiagent reinforcement learning for urban traffic control using coordination graphs. In: Machine Learning and Knowledge Discovery in Databases. Springer, pp. 656–671.
Lauther, U., 2004. An extremely fast, exact algorithm for finding shortest paths in static networks with geographical background. Geoinformation und Mobilität-von

der Forschung zur praktischen Anwendung 22, 219–230.
Leclercq, L., Geroliminis, N., et al., 2013. Estimating mfds in simple networks with route choice. Transport. Res. Part B: Methodol. 57, 468–484.
Leclercq, L., Parzani, C., Knoop, V.L., Amourette, J., Hoogendoorn, S.P., 2015. Macroscopic traffic dynamics with heterogeneous route patterns. Transport. Res. Part C: Emerg. Technol.
Lentzakis, A.F., Su, R., Wen, C., 2014. Time-dependent partitioning of urban traffic network into homogeneous regions. In: 2014 13th International Conference on Control Automation Robotics & Vision (ICARCV). IEEE, pp. 535–540.
Lentzakis, A.F., Su, R., Wen, C., 2016. Strategic learning approach to region-based dynamic route guidance. In: 2016 12th IEEE International Conference on Control and Automation (ICCA). IEEE, pp. 842–847.
Liu, Y., Guo, X., Yang, H., 2009. Pareto-improving and revenue-neutral congestion pricing schemes in two-mode traffic networks. NETNOMICS: Econ. Res. Electron. Network. 10, 123–140.
Mahmassani, H.S., Saberi, M., et al., 2013. Urban network gridlock: theory, characteristics, and dynamics. Proc.-Soc. Behav. Sci. 80, 79–98.
Mazloumian, A., Geroliminis, N., Helbing, D., 2010. The spatial variability of vehicle densities as determinant of urban network capacity. Philos. Trans. Roy. Soc. A: Math. Phys. Eng. Sci. 368, 4627–4647.
Ortigosa, J., Zheng, N., Menendez, M., Geroliminis, N., 2015. Analysis of the 3d-vmfds of the urban networks of zurich and san francisco. In: 2015 IEEE 18th International Conference on Intelligent Transportation Systems (ITSC). IEEE, pp. 113–118.
Ortigosa, J., Zheng, N., Menendez, M., Geroliminis, N., 2017. Traffic performance and road space allocation in multimodal urban networks with an mfd representation. In: Transportation Research Board 96th Annual Meeting.
Papageorgiou, M., 1990. Dynamic modeling, assignment, and route guidance in traffic networks. Transport. Res. Part B: Methodol. 24, 471–495.
Papageorgiou, M., Diakaki, C., Dinopoulou, V., Kotsialos, A., Wang, Y., 2003. Review of road traffic control strategies. Proc. IEEE 91, 2043–2067.
Papageorgiou, M., Messmer, A., 1991. Dynamic network traffic assignment and route guidance via feedback regulation. Transp. Res. Rec. 1306, 49–58.
Ramezani, M., Haddad, J., Geroliminis, N., 2015. Dynamics of heterogeneity in urban networks: aggregated traffic modeling and hierarchical control. Transport. Res. Part B: Methodol. 74, 1–19.
Saeedmanesh, M., Geroliminis, N., 2016. Clustering of heterogeneous networks with directional flows based on snake similarities. Transport. Res. Part B: Methodol. 91, 250–269.
Saeedmanesh, M., Geroliminis, N., 2017. Dynamic clustering and propagation of congestion in heterogeneously congested urban traffic networks. Transport. Res. Proc. 23, 962–979.
Sheffi, Y., 1985. Urban Transportation Network. Equilibrium Analysis with Mathematical Programming Methods. Prentice Hall.
Simoni, M., Pel, A., Waraich, R., Hoogendoorn, S., 2015. Marginal cost congestion pricing based on the network fundamental diagram. Transport. Res. Part C: Emerg. Technol. 56, 221–238.
Sirmatel, I.I., Geroliminis, N., 2016. Model predictive control of large-scale urban networks via perimeter control and route guidance actuation. In: 2016 IEEE 55th Conference on Decision and Control (CDC). IEEE, pp. 6765–6770.
Skabardonis, A., Varaiya, P., Petty, K., 2003. Measuring recurrent and nonrecurrent traffic congestion. Transport. Res. Rec.: J. Transport. Res. Board 118–124.
Small, K.A., Verhoef, E.T., 2007. The Economics of Urban Transportation. Routledge.
Talebpour, A., Mahmassani, H.S., 2016. Influence of connected and autonomous vehicles on traffic flow stability and throughput. Transport. Res. Part C: Emerg. Technol. 71, 143–163.
Tampere, C.M., Corthout, R., Cattrysse, D., Immers, L.H., 2011. A generic class of first order node models for dynamic macroscopic simulation of traffic flows. Transport. Res. Part B: Methodol. 45, 289–309.
Wang, R., Li, Y., Work, D.B., 2017. Comparing traffic state estimators for mixed human and automated traffic flows. Transport. Res. Part C: Emerg. Technol. 78, 95–110.
Xiong, C., Chen, X., He, X., Lin, X., Zhang, L., 2016. Agent-based en-route diversion: dynamic behavioral responses and network performance represented by macroscopic fundamental diagrams. Transport. Res. Part C: Emerg. Technol. 64, 148–163.
Yang, H., 1999. Evaluating the benefits of a combined route guidance and road pricing system in a traffic network with recurrent congestion. Transportation 26, 299–322.
Yen, J.Y., 1971. Finding the k shortest loopless paths in a network. Manage. Sci. 17, 712–716.
Yildirimoglu, M., Geroliminis, N., 2014. Approximating dynamic equilibrium conditions with macroscopic fundamental diagrams. Transport. Res. Part B: Methodol. 70, 186–200.
Yildirimoglu, M., Petit, A., Geroliminis, N., Ouyang, Y., 2016. Bus service design under demand diversion and dynamic roadway congestion based on aggregated network models. In: Transportation Research Board 95th Annual Meeting.
Yildirimoglu, M., Ramezani, M., Geroliminis, N., 2015. Equilibrium analysis and route guidance in large-scale networks with mfd dynamics. Transport. Res. Part C: Emerg. Technol. 59, 404–420.
Zheng, N., Aboudolas, K., Geroliminis, N., 2013. Investigation of a city-scale three-dimensional macroscopic fundamental diagram for bi-modal urban traffic. In: 2013 16th International IEEE Conference on Intelligent Transportation Systems-(ITSC). IEEE, pp. 1029–1034.
Zheng, N., Rérat, G., Geroliminis, N., 2016. Time-dependent area-based pricing for multimodal systems with heterogeneous users in an agent-based environment. Transport. Res. Part C: Emerg. Technol. 62, 133–148.
Zheng, N., Waraich, R.A., Axhausen, K.W., Geroliminis, N., 2012. A dynamic cordon pricing scheme combining the macroscopic fundamental diagram and an agent-based traffic model. Transport. Res. Part A: Policy Pract. 46, 1291–1303.